CHAPTER 3
CATALYST CHARACTERIZATION

CATALYST CHARACTERIZATION

3.1 **Introduction :**

The characterization of catalyst has undergone revolutionary developments in recent years. Powerful novel techniques and instrumentation are now used to analyze catalyst structure, before, during and after use. These developments have resulted in a better understanding of catalytic phenomena and therefore improvements in commercial catalysts and the discovery of new systems. The application of advanced electronics and computer analysis has optimized many of these analytical tools. Thus, the difficult goal of unravelling the relationship between the structure and reactivity of catalytic materials is finally within reach.

However, the complete characterization of supported catalysts is extremely difficult due to the inhomogeneous nature of the catalyst themselves. Accordingly a wide range of analytical and spectroscopic techniques have been applied to the problem (1-2).

The characterization of a catalyst provides information on three distinct but related sorts. They are : chemical composition and chemical structure, texture and mechanical properties and catalytic activity.

Chemical composition and chemical structure refer to the elemental composition, proportions of individual phases present, surface composition, nature and properties of surface functional groups. The structure of a catalyst refers to its geometric structure and morphology. The

characterization of a catalyst in terms of its activity is a quantitative measure of the ability of the catalyst to carry out a particular chemical transformation under specified conditions.

A typical characterization of a supported metal complex would include the study of physico-chemical nature of the support, followed by a careful record of the conditions under which the supported catalyst has been prepared. Micro analysis for many of the elements present and application of spectroscopic techniques to study the response of supported catalysts to probe molecules such as CO, H_2 and NO. All the approaches put together help to arrive at the possible structure of the metal complex on the polymer.

Present chapter deals with the physico-chemical characterization of polymer bound and unbound complexes such as, chemical composition, moisture content, apparent bulk density, surface area and swelling studies. Spectroscopic studies have been utilized to investigate the co-ordination structure of polymer bound metal complexes, oxidation state of the central metal atom and the morphology of the supported metal complex catalysts using techniques such as UV-Visible spetra, IR, FTIR, NMR, ESCA and SEM. Thermal stability of the support and supported complexes have been studied using DTA and TG analysis. Based on the spectroscopic and physico-chemical characteristics, the schemes have been proposed for the possible structures of metal complexes on the polymer matrices.

3.2 **Apparent bulk density and moisture content :**

Apparent bulk density and percentage of moisture content of all the catalysts are given in Table 3.1. Bulk density and percent moisture content of the catalysts were found to increase with a decrease in percent crosslinking of the polymer support. The percent moisture for Ruthenium catalysts was found to be more than that of palladium catalysts. Since the polymer (Polystyrene - DVB) support is hydrophobic in nature (3), the similar nature of the supported catalysts may be attributed either due to hydrogen bonding of water with amino groups or co-ordination with metal atom.

Table 3.1

Moisture content and apparent bulk density of the catalysts.

Catalyst	Moisture content (Wt%)	Apparent bulk density (gml^{-1})
5PRu(III)DAP	1.62	0.45
15PRu(III)DAP	1.28	0.50
5PPd(II)DAP	1.51	0.49
15PPd(II)DAP	1.22	0.46
2XRu(III)DAP	0.40	0.37
2XPd(II)DAP	0.38	0.36
8XRu(III)DAP	0.32	0.39
8XPd(II)DAP	0.30	0.38

The apparent bulk density is an important practical parameter because it indicates the mass of catalyst which will be packed into a reactor of specified volume when the polymer supported catalyst is employed in a liquid phase slurry reactor. This parameter will not play any significant role, because the volume occupied by swollen polymer is more than the dry polymer and the swelling capacity differs from solvent to solvent. However when the catalyst is used in a vapour phase reactor, it will be a useful parameter.

3.3 **Chemical composition :**

Elemental analysis of carbon, hydrogen, nitrogen, chloride and metal content for ruthenium and palladium complexes of 1,2-diaminopropane at various stages of reaction are given in Tables 3.2 - 3.3. The number of ligand molecules attached with the polymer were calculated by the difference of two chloride ion contents (estimated gravimetrically) before and after introduction of ligand. The calculated and experimental values were found to be in close agreement. Low loading of the metal and hence the chelation on the polymer matrix was achieved by carrying out the complexation reaction under mild conditions in presence of a good swelling agent. It is obvious that the polymer complex formation represents a complicated process. The polymer matrix swells after absorbing the solvent which changes the polymer structure. The swollen polymer then interacts with the metal ions and the complex formation takes place. It may be taken into account that each functional group (ligand)

Table 3.2

Elemental analysis and metal loading at different stages of catalyst preparation.

Catalyst	A			B			C			
	C(WT%)	H(WT%)	Cl(WT%)	C(WT%)	H(WT%)	N(WT%)	C(WT%)	H(WT%)	N(WT%)	Ru(WT%)
5P Ru(III) DAP	76.18	7.31	9.8	72.20	7.48	2.73	71.62	7.28	2.51	3.75×10^{-2}
15P Ru(III) DAP	87.21	7.35	8.9	84.21	7.40	2.59	83.92	7.36	2.53	3.25×10^{-2}
2X Ru(III) DAP	62.77	7.47	5.7	61.01	7.28	1.68	61.76	7.35	1.44	3.2×10^{-3}
8X Ru(III) DAP	84.28	7.01	4.8	83.33	6.98	1.77	82.88	6.77	1.53	1.57×10^{-3}

A = After Chloromethylation

B = After ligand introduction

C = After complex formation.

Table 3.3

Elemental analysis and metal loading at different stages of catalyst preparation.

Catalyst	A			B			C			
	C(WT%)	H(WT%)	Cl(WT%)	C(WT%)	H(WT%)	N(WT%)	C(WT%)	H(WT%)	N(WT%)	Pd(WT%)
5P Pd(III) DAP	75.98	7.24	9.8	71.23	7.33	2.22	71.11	7.18	2.09	4.35×10^{-2}
15P Pd(III) DAP	86.41	7.32	8.9	85.11	7.36	2.12	84.98	7.08	1.89	3.9×10^{-2}
2X Pd(III) DAP	62.86	7.42	5.7	61.26	7.31	1.80	61.52	7.28	1.61	2.2×10^{-3}
8X Pd(III) DAP	83.92	6.99	4.8	83.42	6.52	1.66	82.42	6.81	1.33	2.1×10^{-3}

A = After Chloromethylation

B = After ligand introduction

C = After complex formation.

comes in contact with metal ions and co-ordinates with this to form "inner coordination complex". Then the spacial arrangement of the complexing groups over the polymer ligand chain takes various orientations with respect to the main chain. As a result, the total polymer complex as a whole is formed. The polymer complex formation also represents a relaxation process, which is related to the probability of transition of the system from one state of equilibrium to another.

3.4 **Surface area measurement :**

The total surface area of the supports and catalysts were measured using non-specific physical adsorption method. (4,5) Adsorption -desorption isotherms of nitrogen were recorded on a Carlo-Erba Sorptiomatic series - 1900 at 196° C (liquid N_2 temp) after degassing the sample at 80° C for 4 hours. From the isotherms specific surface area and pore volume were calculated using BET equation.

It is found that in the case of 5% and 15% styrene - DVB the surface area reduces by $\simeq$ 1 m^2g^{-1} after anchoring the complexes while in the case of XAD-2 and XAD-8 it reduces considerably. The results are given in Tables 3.4 and 3.5. A decrease observed in the surface area may be due to blocking of pores of the support by the successive introduction of chloromethyl groups, ligand and formation of metal complex on the polymer matrix.

Table 3.4

Surface area and pore volume of supports.

Polymer support	Surface area ($m^2 g^{-1}$)	Pore volume (ml g^{-1})
5 %	9.781	0.212
15 %	27.932	0.425
XAD-2	330.00	0.420
XAD-8	160.00	0.525

Table 3.5

Surface area and pore volume of catalysts.

Catalyst	Surface area ($m^2 g^{-1}$)	Pore volume (ml g^{-1})
5 P Ru(III) DAP	8.721	0.209
5 P Pd(III) DAP	8.824	0.217
15P Ru(III) DAP	26.842	0.398
15P Pd(III) DAP	26.972	0.402
2 x Ru(III) DAP	298.420	0.420
2 x Pd(III) DAP	304.472	0.421
8 x Ru(III) DAP	149.602	0.569
8 x Pd(III) DAP	152.812	0.572

3.5 **Swelling studies :**

In-order to optimise both the rate and specificity of a particular catalyst system it is necessary to consider many factors. The nature of the solvent used plays an important role in the rate of the reaction. Polymer swelling is a very useful parameter to control both specificity and selectivity in a batch reactor. It becomes undesirable in a fixed bed reactor as it leads to blocking of the inter bead channels and so prevents flow through the reactor bed.

To achieve higher activity and selectivity with polymer bound catalysts, it is necessary that the reactant molecules have accessibility to all catalytic sites both on the surface and interior of the beads. This could be achieved with a solvent in which the polymer support has a maximum swelling so that the matrix expands sufficiently to allow the reactant molecules to diffuse within the solvent channel and encounter the catalytic centres.

The extent of swelling with a particular solvent depends upon the groups attached to the polymer matrix. An exhaustive study of swelling has been done with nine different solvents of various nature (i.e., aliphatic, aromatic, polar and non-polar) for the support as well as the catalysts. The results are given in Tables 3.6 and 3.7. The plot of polymer crosslink vs mole percent of swelling is given in Figs. 3.1 and 3.2 for catalysts.

Table 3.6

Swelling studies of polymer bound ruthenium catalysts in different solvents.

Solvent	Swelling in Mole %			
	5P Ru(III) DAP	15P Ru(III) DAP	2X Ru(III) DAP	8X Ru(III) DAP
Water	0.728	0.692	1.210	0.962
Methanol	0.678	0.611	0.621	0.610
Ethanol	0.471	0.402	0.614	0.601
Dioxane	0.211	0.198	0.512	0.497
DMF	0.142	0.137	0.502	0.442
Acetone	0.128	0.110	0.486	0.420
THF	0.108	0.098	0.481	0.411
Benzene	0.102	0.086	0.321	0.308
n-Heptane	0.058	0.040	0.109	0.095

Table 3.7

Swelling studies of polymer bound palladium catalysts in different solvents.

Solvent	Swelling in Mole %			
	5P Pd(II) DAP	15P Pd(II) DAP	2x Pd(II) DAP	8x Pd(II) DAP
Water	0.711	0.658	1.18	0.941
Methanol	0.596	0.592	0.586	0.410
Ethanol	0.388	0.362	0.562	0.400
Dioxane	0.122	0.116	0.507	0.367
DMF	0.112	0.103	0.478	0.358
Acetone	0.101	0.092	0.416	0.321
THF	0.094	0.084	0.392	0.290
Benzene	0.079	0.060	0.294	0.256
n-Heptane	0.039	0.031	0.095	0.092

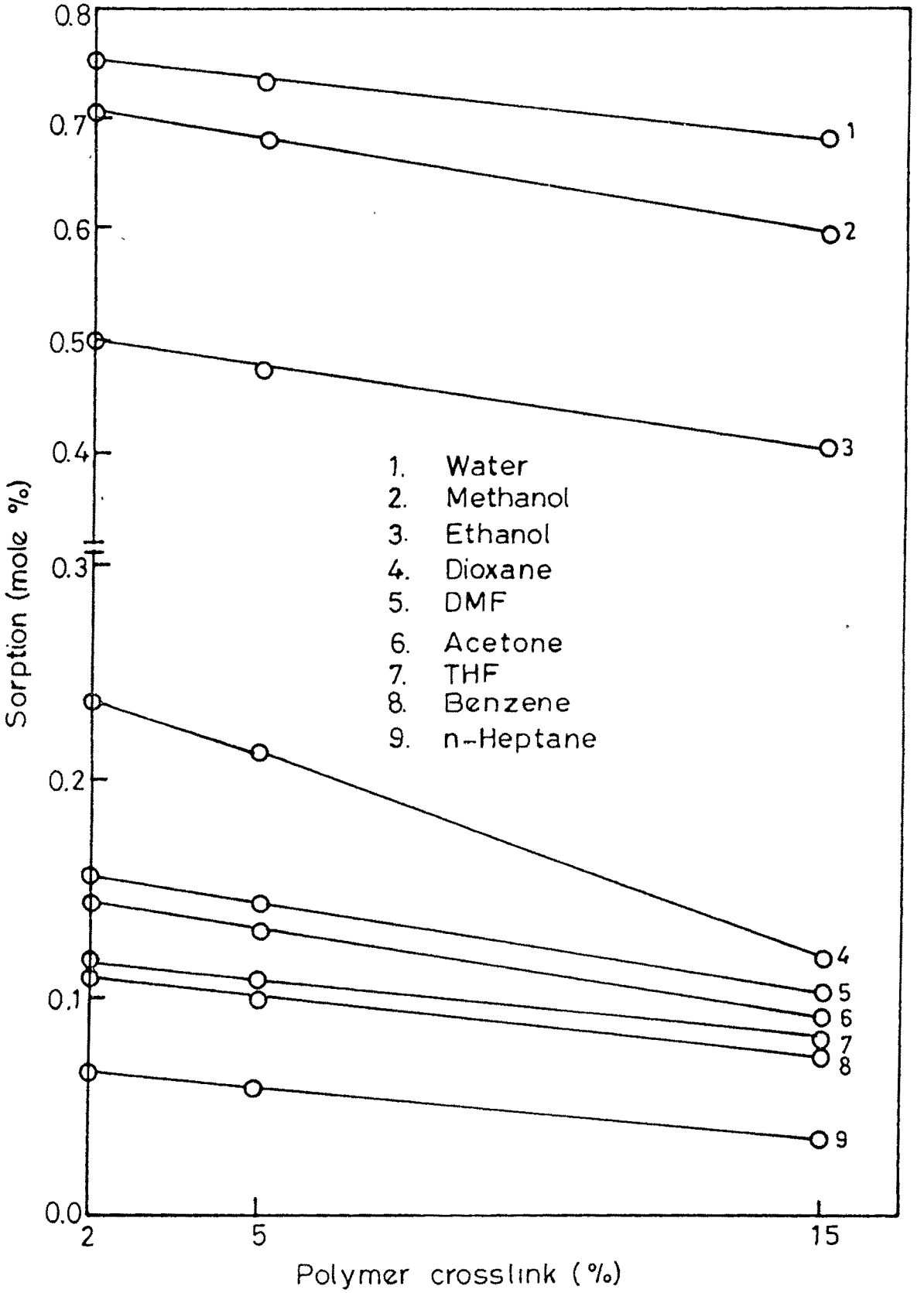

Fig. 3.1 Swelling studies of polymer supported ruthenium catalysts

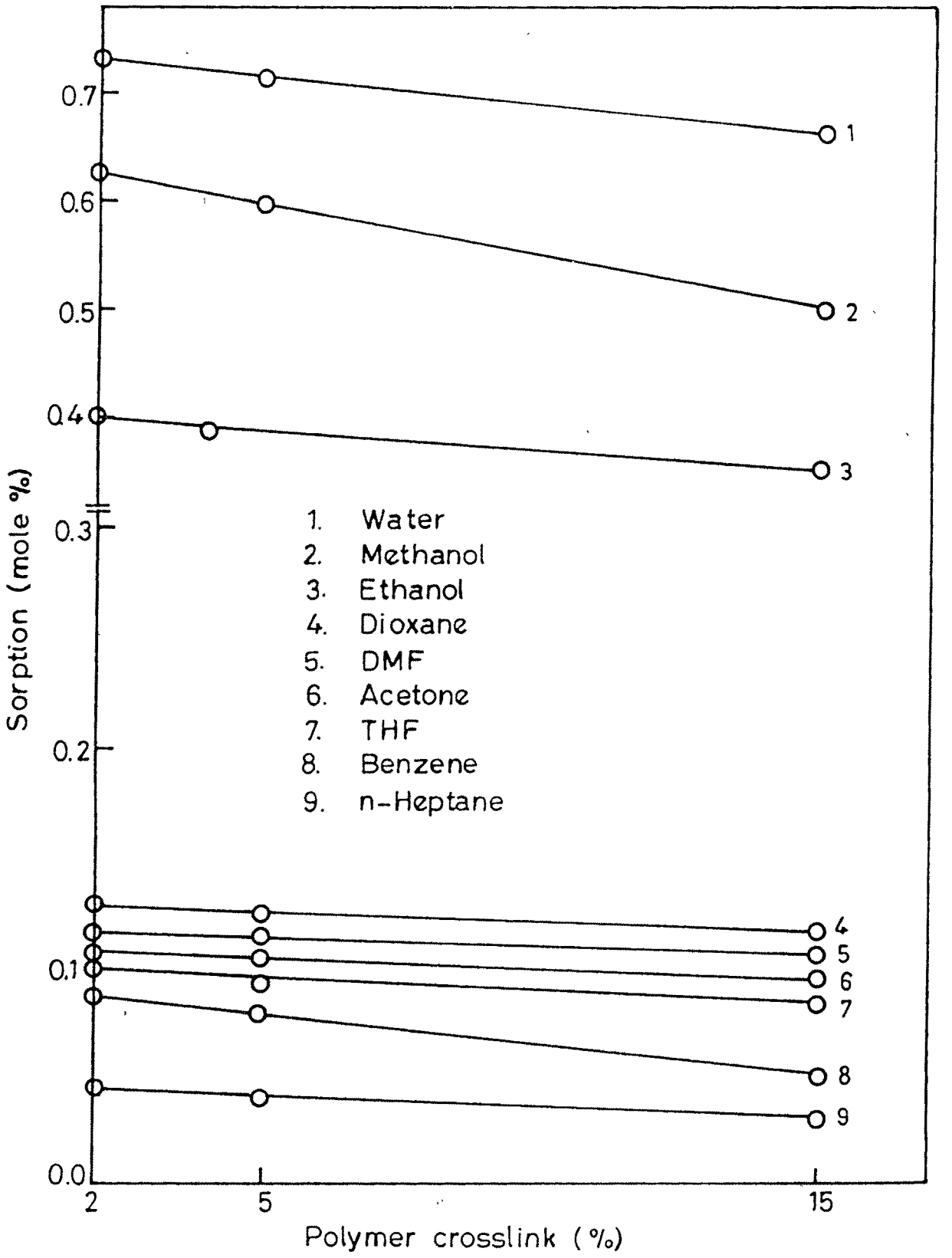

Fig. 3.2 Swelling studies of polymer supported palladium catalysts

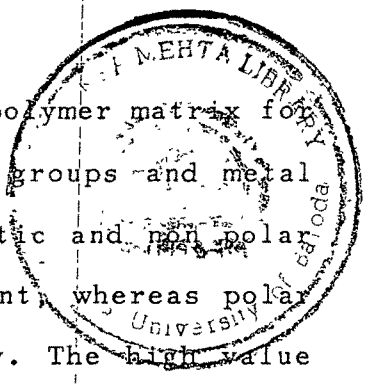

It is found that the affinity of the polymer matrix for different solvents changes when functional groups and metal atoms are incorporated into it. Thus aliphatic and non polar solvents were found to be poor swelling agent, whereas polar solvents have the maximum swelling capacity. The high value of swelling percent in water may be due to the hydrogen bonding of water molecules with amino groups. However for the sake of comparison of catalytic activity of all the catalysts a common solvent methanol is chosen as the reaction medium.

3.6 Spectral characterization (6-9) :

3.6.1 UV-Visible spectroscopy :

The interaction of light with catalyst particles has been a major tool in the characterization of catalysts. The transitions involved in UV-Visible region are electronic. Thus d-d transitions are observable when degenerate d-orbitals are split by placing a transition metal ion in a crystal field. The splitting of the energy levels is affected by the number of d-electrons, the effective charge on the ion, the distribution and the charge of the surrounding ions. These transitions usually occur in the visible part of the spectrum. Charge transfer transitions involve more than one atom and include transitions from metal to ligand or vice versa, or between two neighbouring metal atoms of different oxidation states. Usually such transitions occur in the UV region and do not mask the d-d transitions in the visible region. The technique employed in UV-Visible spectroscopy for

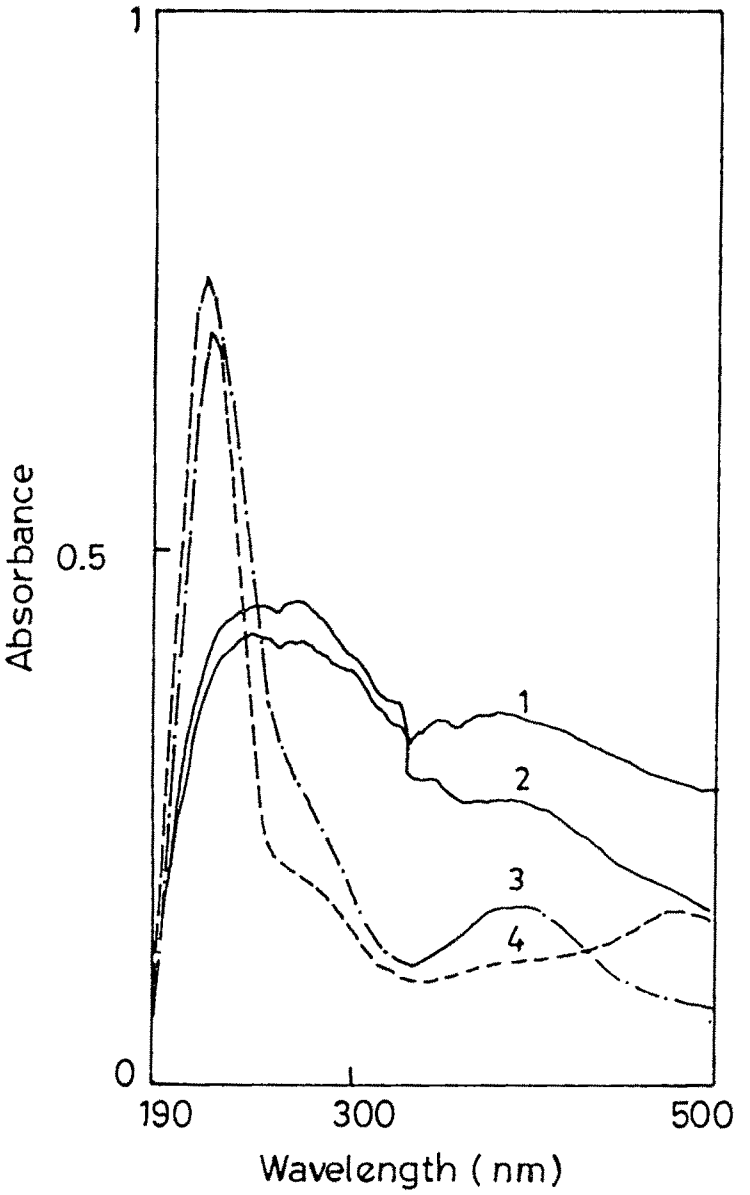

Fig. 3.3 UV-Vis reflectance spectra of
1. 15PRu(III)DAP 2. 15PPd(II)DAP
3. 8XPd(II)DAP 4. 8XRu(III)DAP

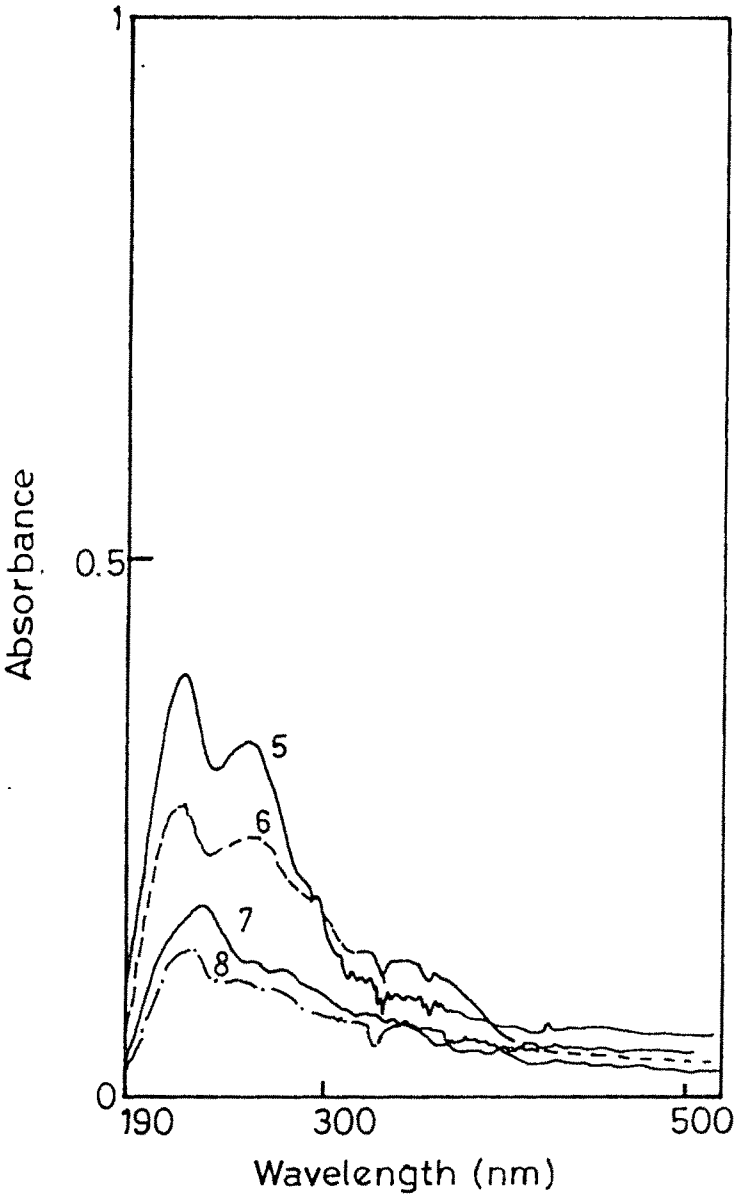

Fig. 3.4 UV-Vis refletance spectra of

5. 2XRu(III)DAP 6. 2XPd(II)DAP
7. 5PRu(III)DAP 8. 5PPd(II)DAP

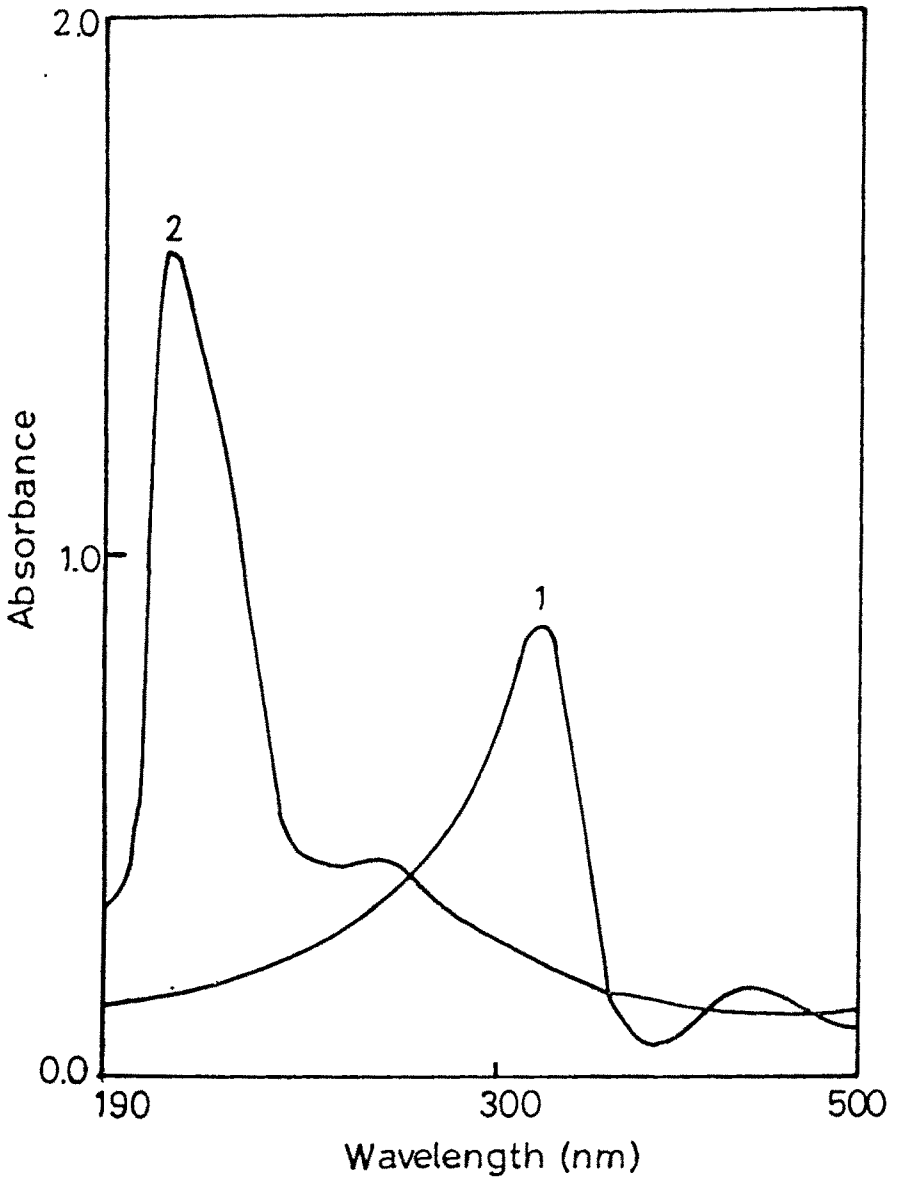

Fig. 3.5 UV-Vis absorbance spectrum of
1. [PdDAP]Cl_2 2. [RuDAPCl_2]Cl in methanol

powdered samples involve the measurement of diffusely reflected light (7).

Figs. 3.3 and 3.4 shows the UV-Visible diffuse reflectance spectra recorded for the polymer bound ruthenium and palladium catalysts using $BaSO_4$ as standard. In the case of polymer bound ruthenium complexes, the broad absorption band including three peaks between 210 and 500 nm was assigned to d-d transitions of Ru(III) and for palladium (II), the absorption bands appeared at 340 nm and 430 nm.

Fig 3.5 shows the UV-Visible spectra of unbound [Ru DAP Cl_2]Cl and [Pd DAP]Cl_2 in methanol and the absorption maxima was found to be 210 nm [10] and 340 respectively.

3.6.2 **Infrared spectroscopy :**

Infrared spectroscopy has been frequently used for the study of adsorbed molecule and of their binding with catalyst surface. It provides a reliable information about the organic compounds in the IR (i.e., 600 - 4000 cm^{-1}) region and that of metal ligand vibrations in Far - IR (50 - 600 cm^{-1}) region. The formation of metal complex, the bond formed between the metal and co-ordinating atom of the ligand molecule can be understood by the nature and position of the absorption bands.

Absorption spectra of polymer bound ligands or metal ions are changed some times drastically by complex formation.

The macromolecular chain adjacent to the co-ordinating group influences the absorption band in the spectra. Hence the spectra will be dependent on the nature of the polymer chain.

It was observed that the spectra of polymer bound complexes are complicated and interpretation of just a polymer bound catalyst will always be misleading. Hence a detailed study of absorption spectra of polymer support, functionalized support, polymer bound metal complex has been made for conclusive information.

Infrared spectra of crosslinked polystyrene chloromethylated polymer, liganded polymer and the catalysts are given in Figures. 3.6 to 3.11

The IR absorption frequency of a ligand is usually shifted by complex formation with metal atom (11 - 12).

A summary of the IR frequency assignment for the catalysts are given in Tables 3.8 and 3.9. It is observed from the micro analysis and metal loading that all the attached ligand molecules are not involved in complex formation. Even then, the formation of metal chelates could be concluded from the decrease in intensities of amino absorption bands in the region 3400 - 3500 cm^{-1} and also from the appearente of new bands due to chelation.

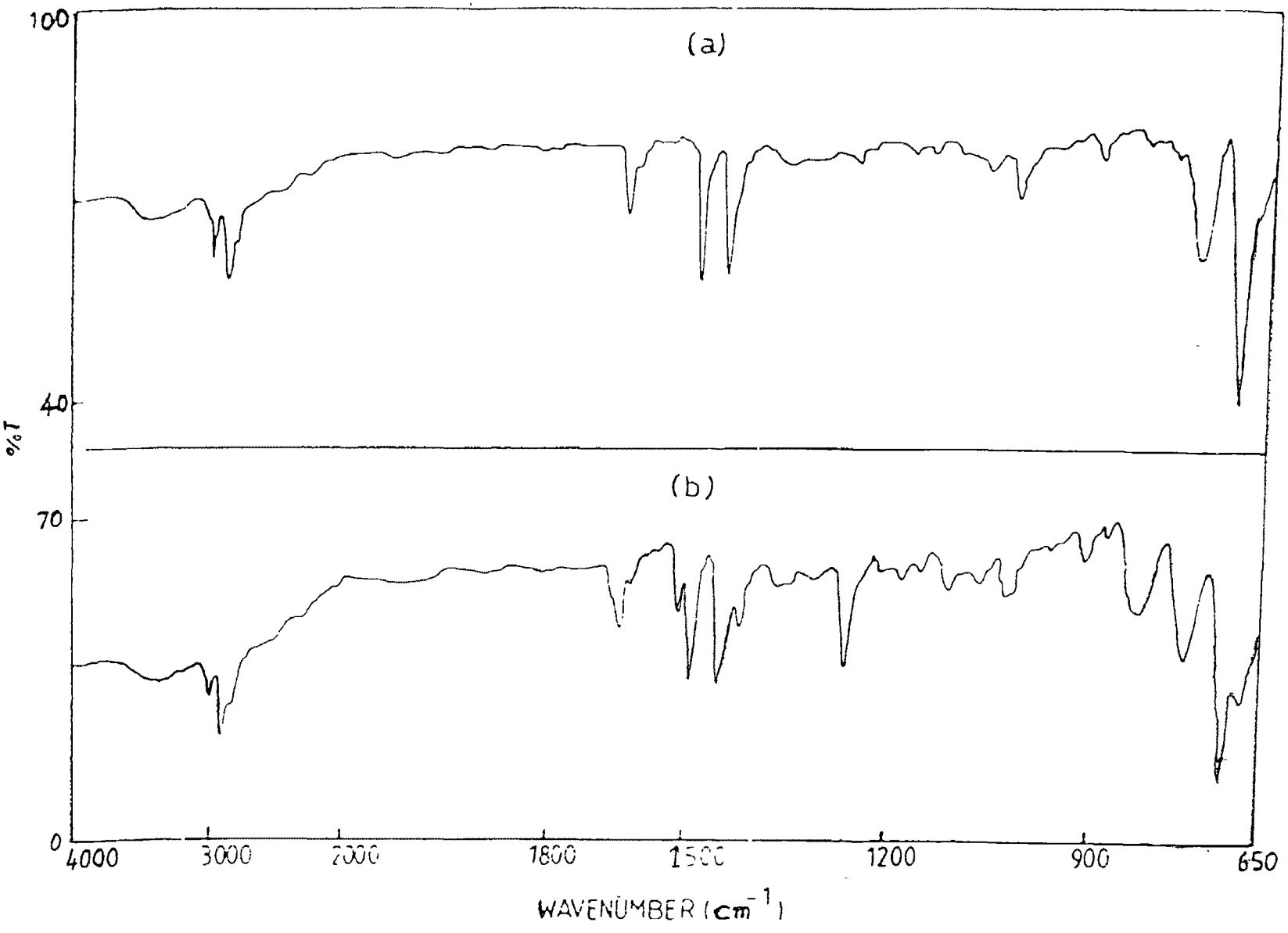

Fig. 3.6 Infrared spectra of a. 5% crosslinked poly (Sty-DVB) b. Chloromethylated 5P

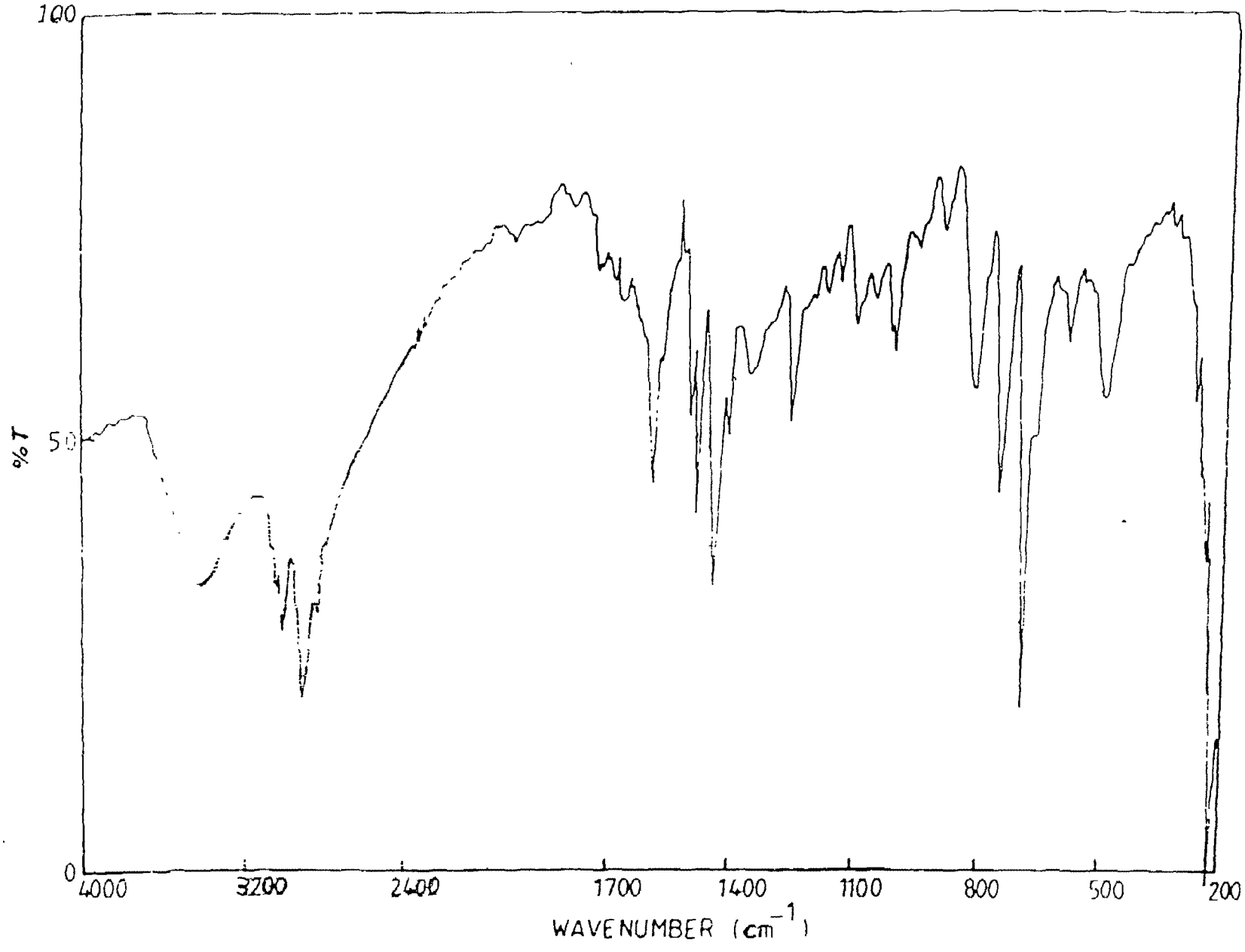

Fig. 3.7 Infrared spectrum of liganded polymer i.e., 5PDAP

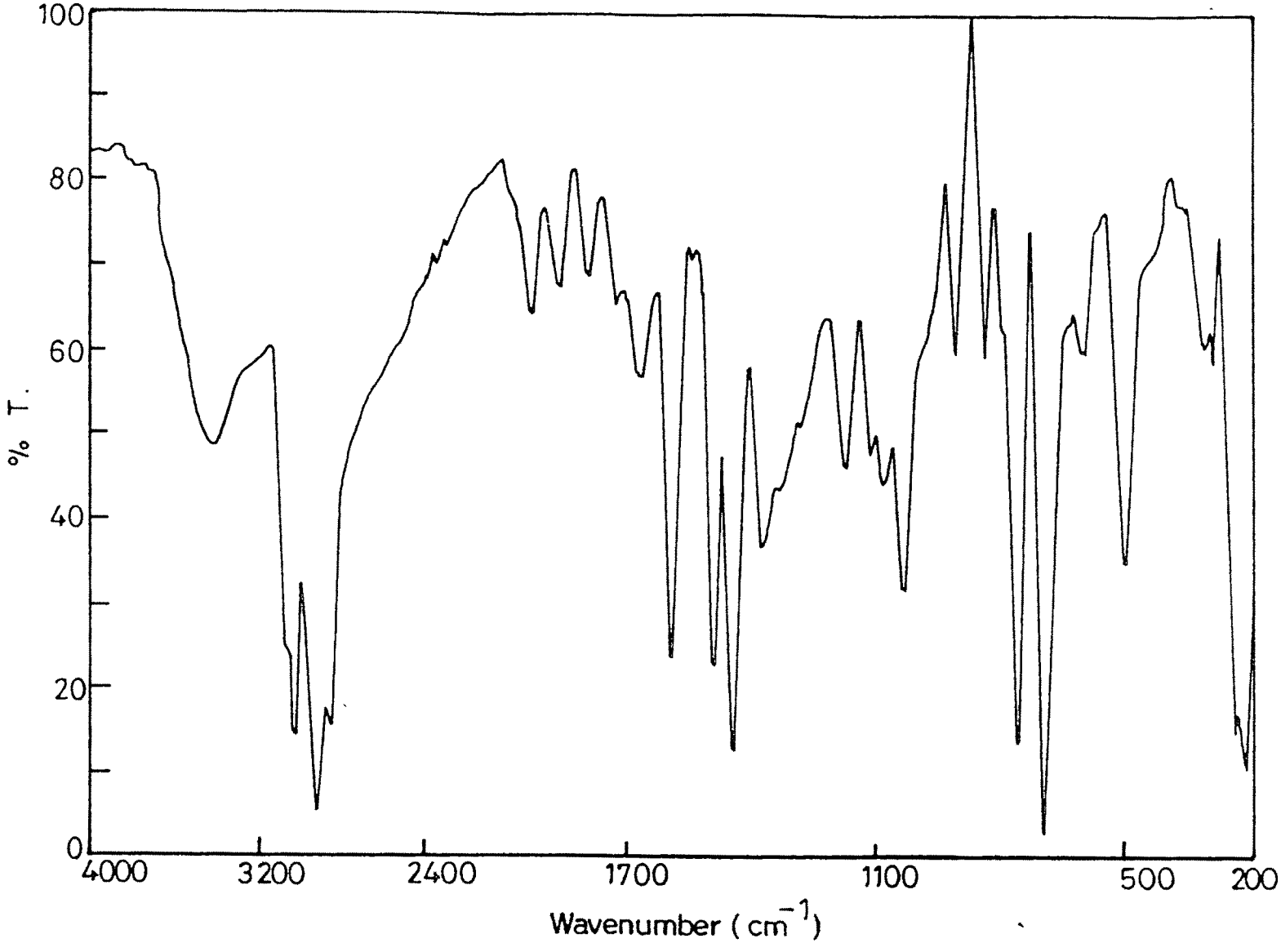

Fig. 3.8 Infrared spectrum of the catalyst 15PPd(II)DAP

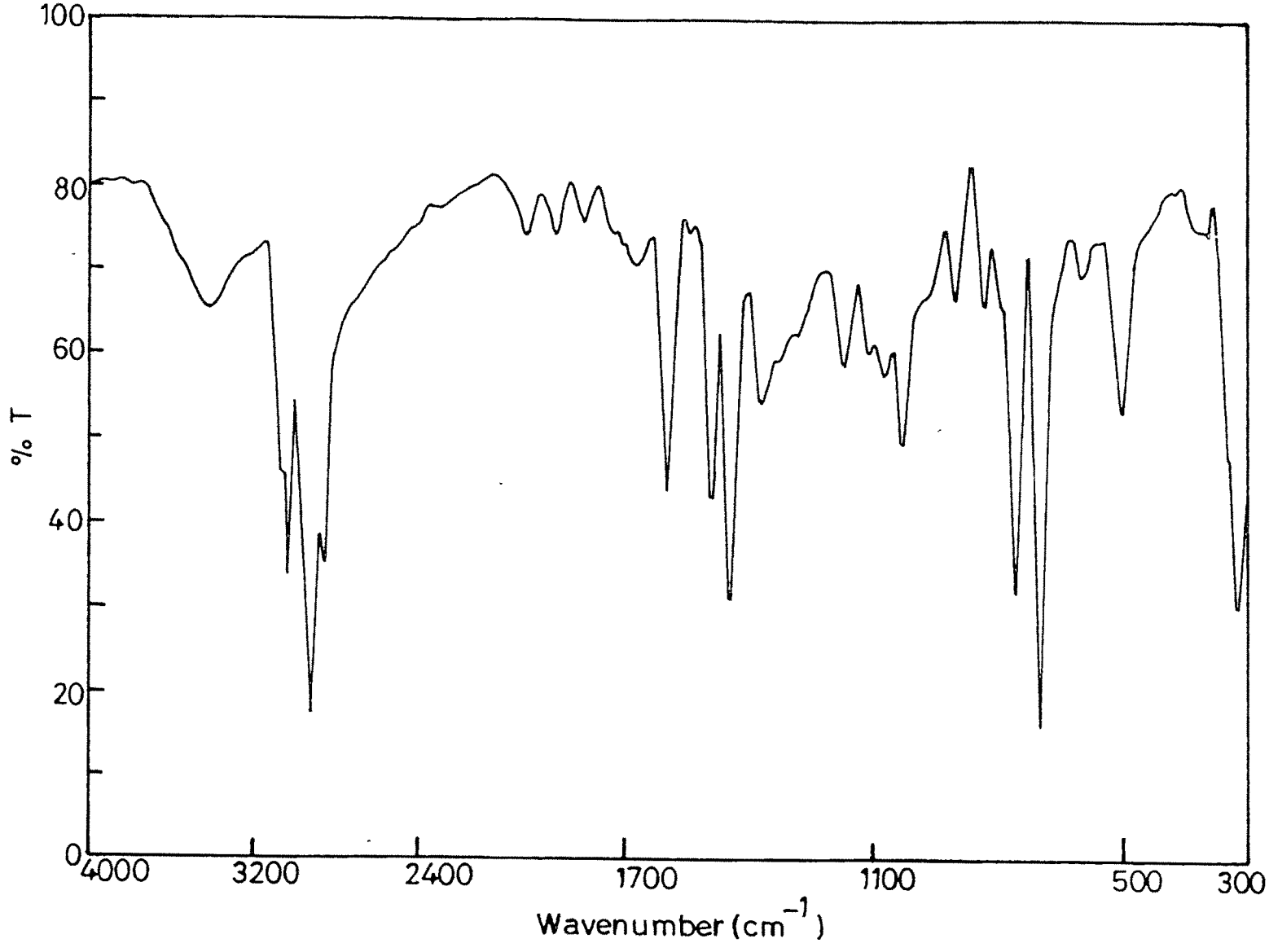

Fig. 3.9 Infrared spectrum of the catalyst 15PRu(III)DAP

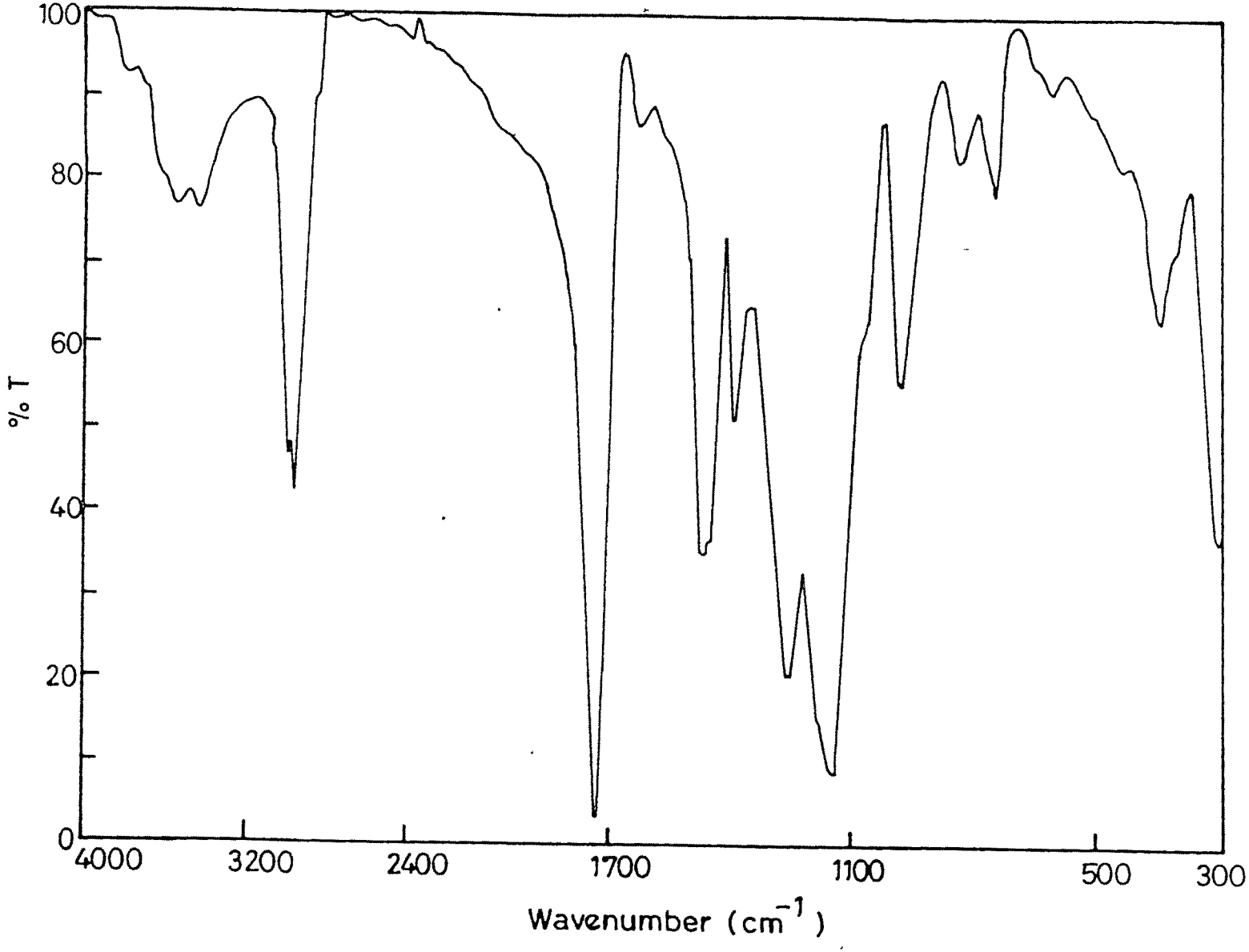

Fig. 3.10 Infrared spectrum of the catalyst 8XPd(II)DAP

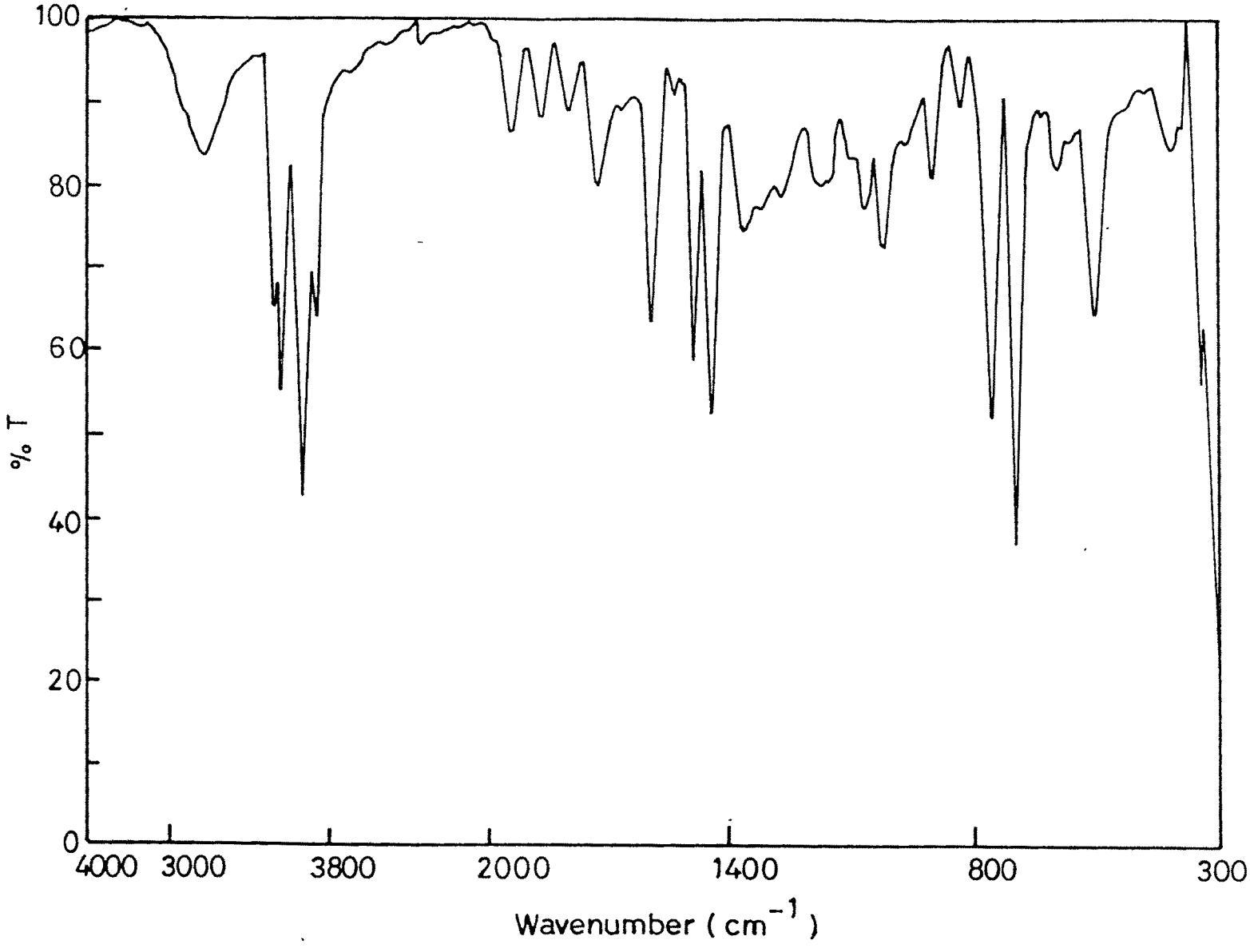

Fig. 3.11 Infrared spectrum of the catalyst 8XRu(III)DAP

Table : 3.8

A summary of the IR frequency assignment for polymer bound ruthenium catalysts.

Catalyst	Ru-Cl Str$_{-1}$ (cm^{-1})	Ru-N Str$_{-1}$ (cm^{-1})	C-N Str$_{-1}$ (cm^{-1})	N-H Str$_{-1}$ (cm^{-1})	$-CH_2Cl$ Str$_{-1}$ (cm^{-1})
5PRu(III)DAP	250	320	1030	3420 1603	1265
15PRu(III)DAP	225	300	1072	3407 1598	1170
2XRu(III)DAP	241	322	1044	3440 1602	1271
8XRu(III)DAP	240	314	1069	3437 1633	1272

Table : 3.9

A summary of the IR frequency assignment for polymer bound palladium catalysts.

Catalyst	Pd-Cl Str$_{-1}$ (cm^{-1})	Pd-N Str$_{-1}$ (cm^{-1})	C-N Str$_{-1}$ (cm^{-1})	N-H Str$_{-1}$ (cm^{-1})	$-CH_2Cl$ Str$_{-1}$ (cm^{-1})
5PPd(II)DAP	310	504	1107	3406 1502	1266
15PPd(II)DAP	312	497	1073	3424 1599	1168
2XPd(II)DAP	322	506	1043	3440 1602	1265
8XPd(II)DAP	347	499	1151	3443 1630	1260

3.6.3 **FTIR Spectroscopy :**

The principal advantage of FT-IR over disperse IR lies in the much higher signal to noise ratio which can be obtained by FT technique. The FTIR has a number of significant intrinsic advantages over disperse -IR (12a), improving the performance of IR enormously. FTIR has a strong aperture advantage because the aperture can be made larger than the corresponding slit in the monochromator. Dispersive IR spectrometers do not allow this. Thus, the quantity of light incident on the inter -ferometer is much greater than that on a monochromator. Since all signals are modulated, the effect of stray light is negligible in FTIR. Hence FTIR has emerged as a fast and sensitive technique which is well suited for catalyst studies. The FTIR spectra of all the polymer supported catalysts are given in Figures 3.12 to 3.19; tables 3.10 and 3.11 show the FT-IR frequency assignment.

3.6.4 **Nuclear magnetic resonance spectroscopy (NMR) :**

Proton magnetic resonance has not been used for structural analysis of polymer complex because its solubility is usually low and the complexation of polymer ligand with metal ion often leads to broadening of the spectrum. In general, complex formation with metal ion leads to shift, splitting, or broadening of the peaks due to ligand molecule.

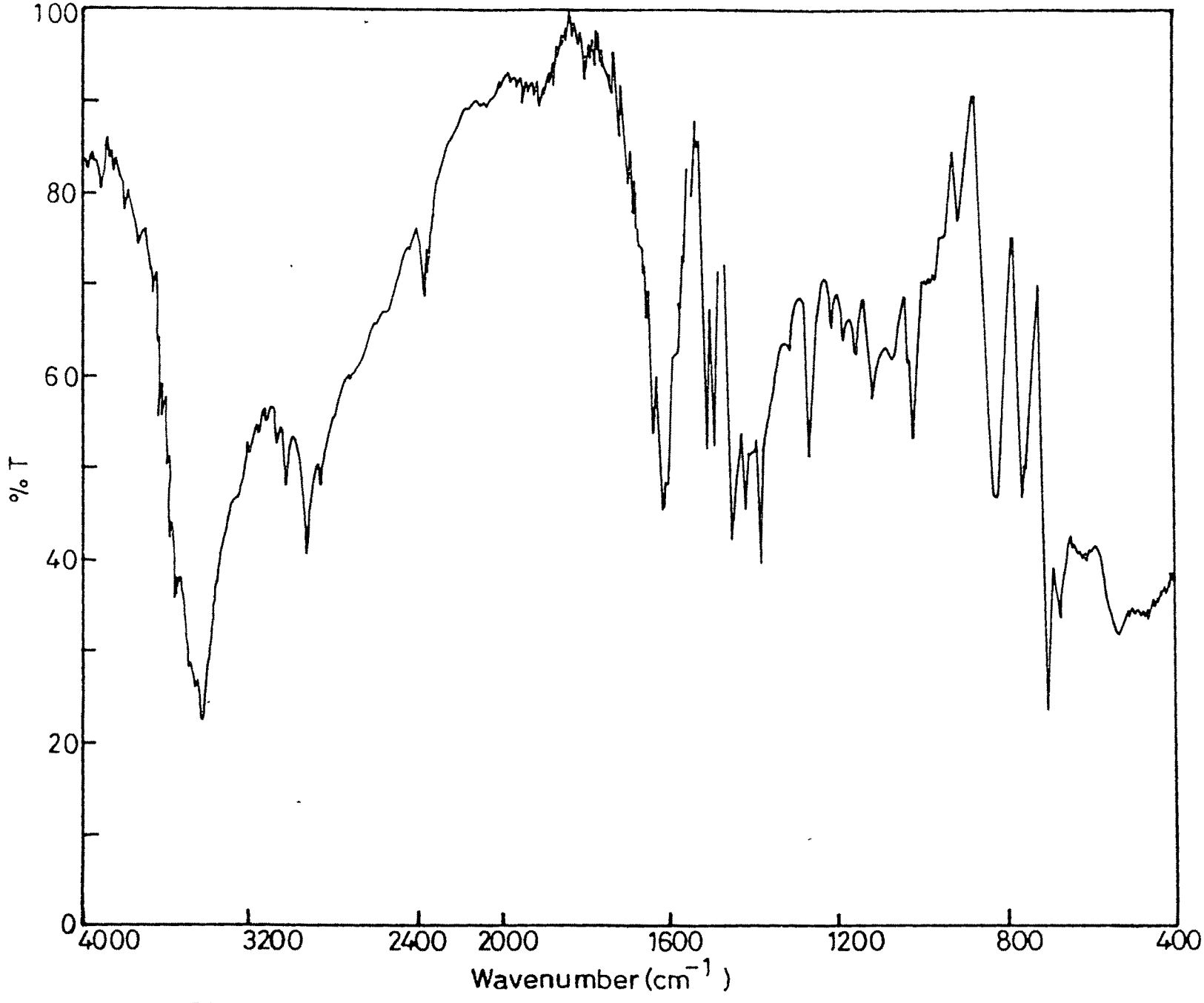

Fig. 3.12 FT-IR spectrum of the catalyst 5PRu(III)DAP

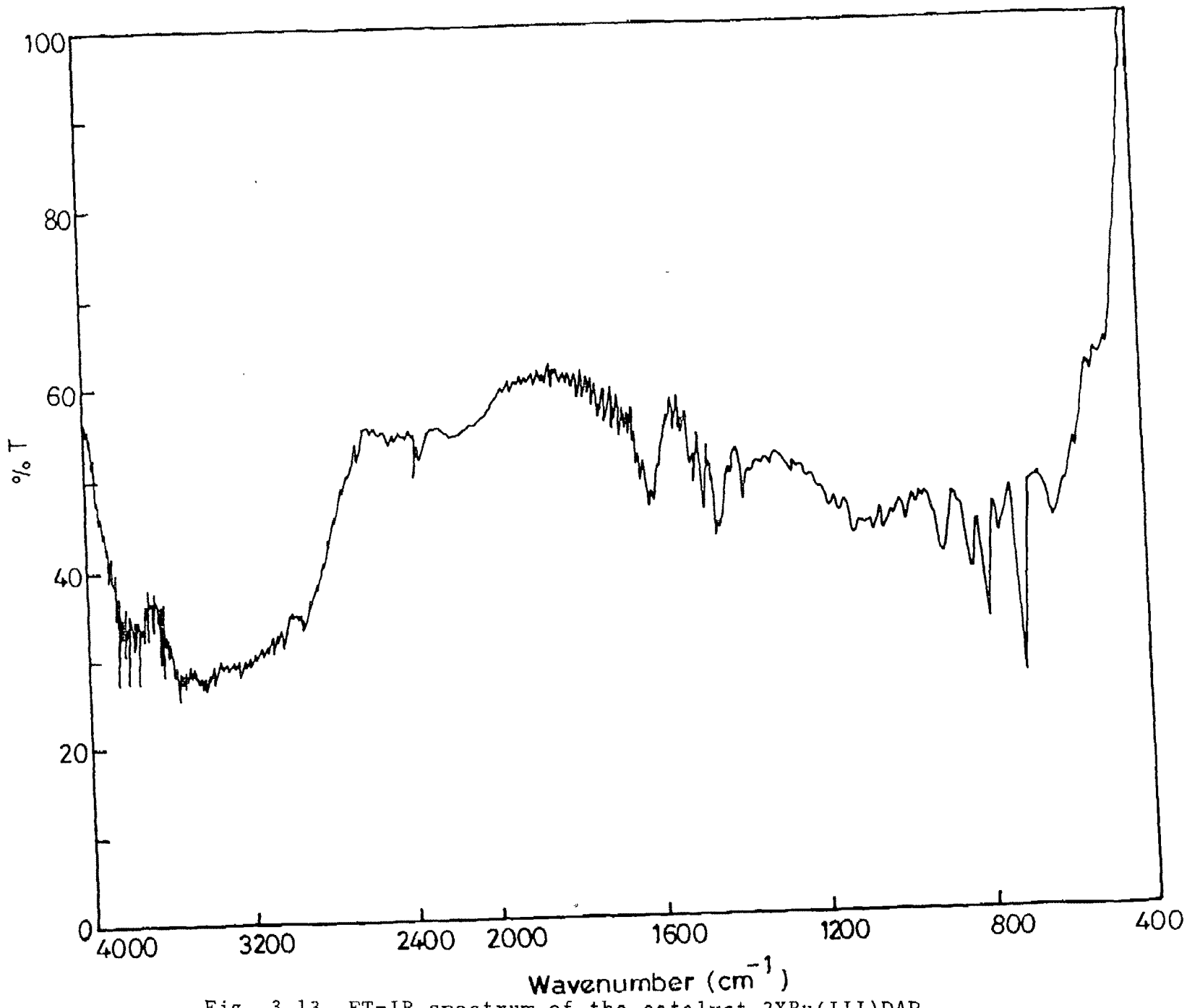

Fig. 3.13 FT-IR spectrum of the catalyst 2XRu(III)DAP

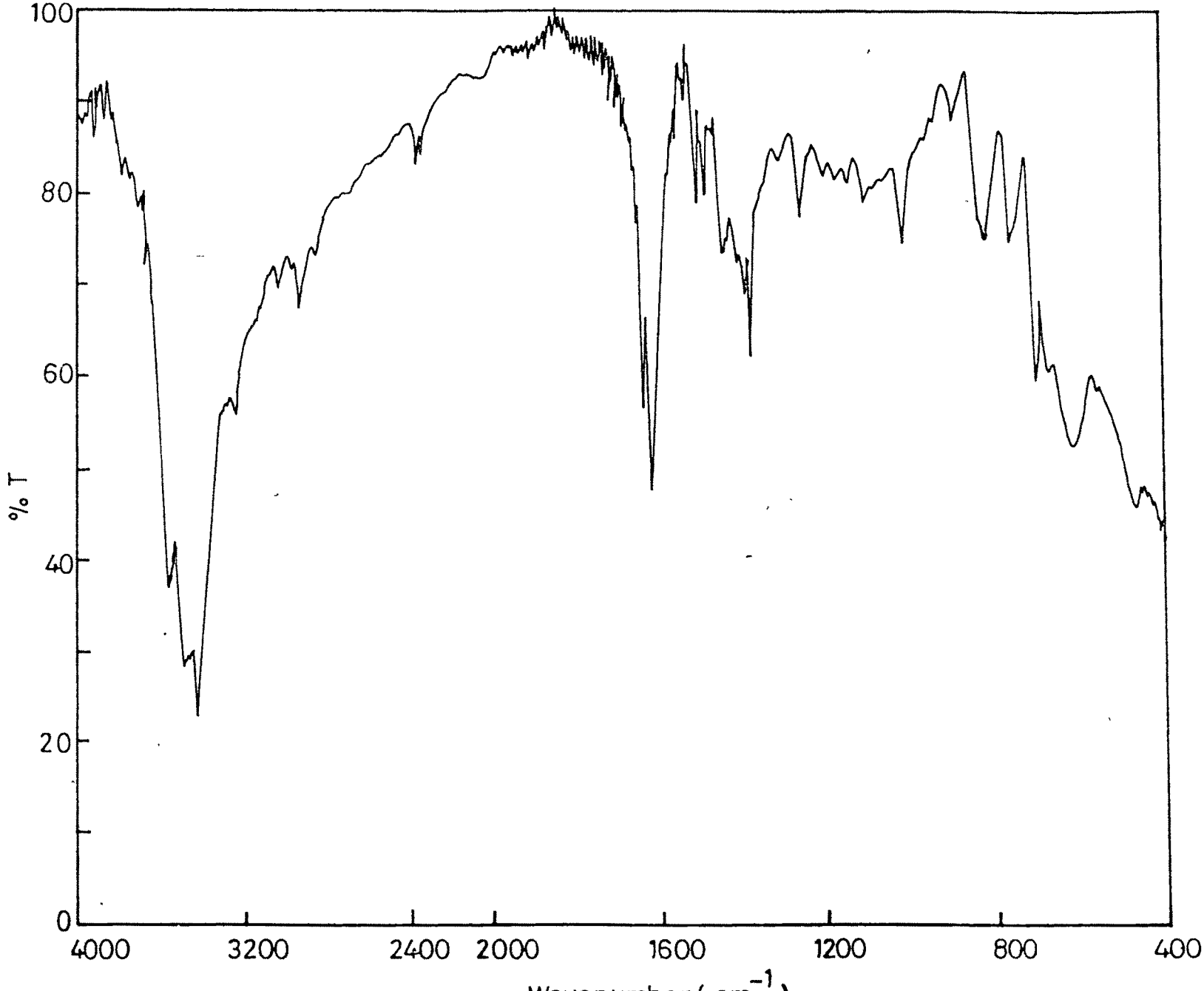

Fig. 3.14 FT-IR spectrum of the catalyst 5PPd(II)DAP

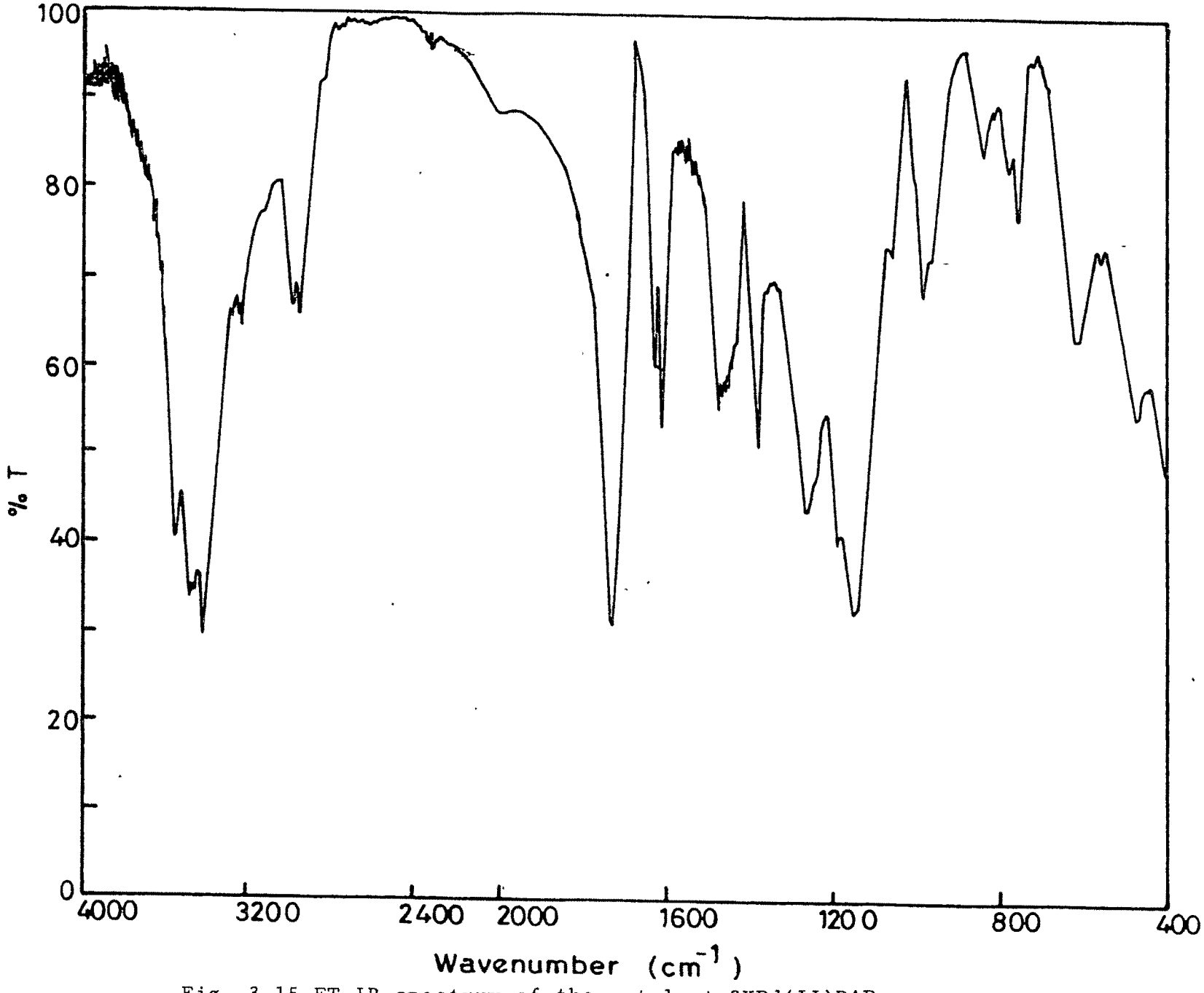

Fig. 3.15 FT-IR spectrum of the catalyst 2XPd(II)DAP

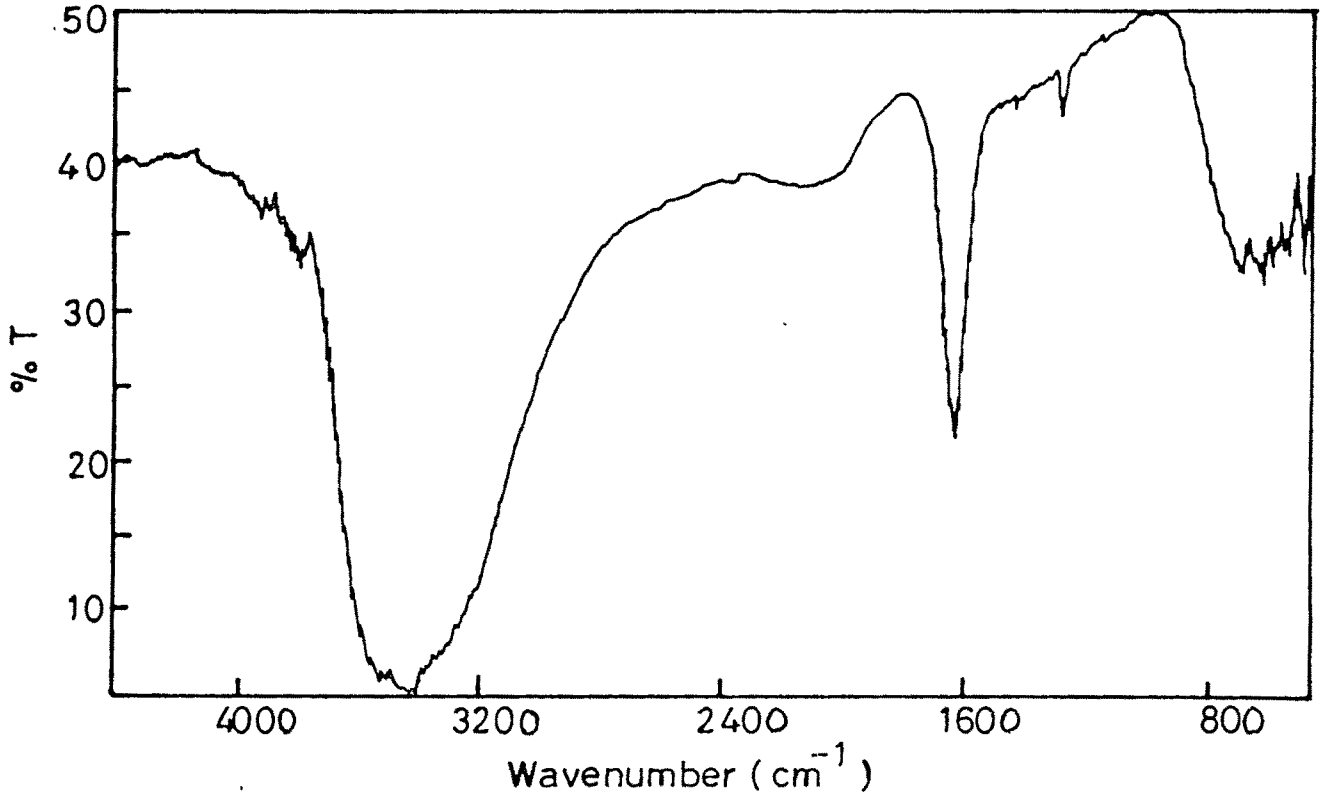

Fig.3.16 FT-IR spectrum of the catalyst 15PRu(III)DAP

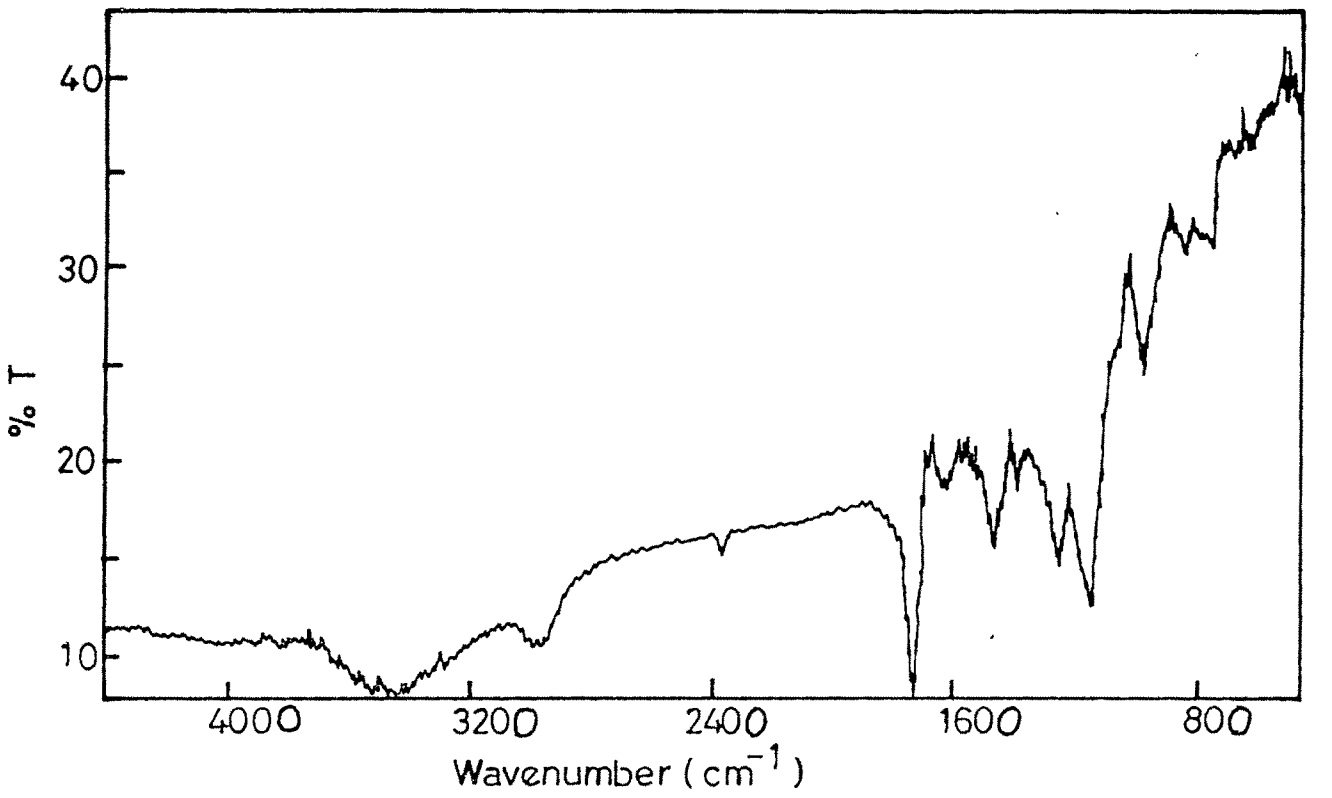

Fig. 3.17 FT-IR spectrum of the catalyst 8XRu(III)DAP

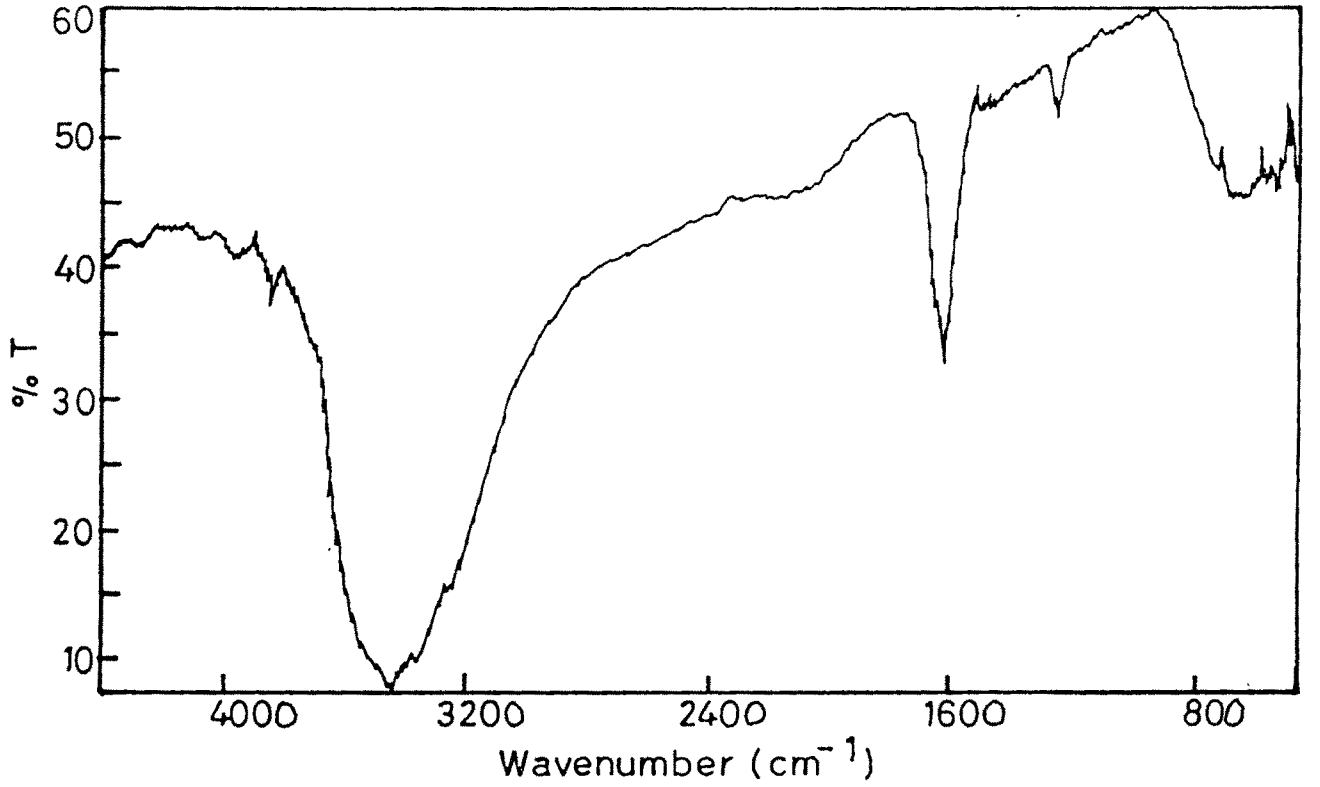

Fig. 3.18 FT-IR spectrum of the catalyst 15PPd(II)DAP

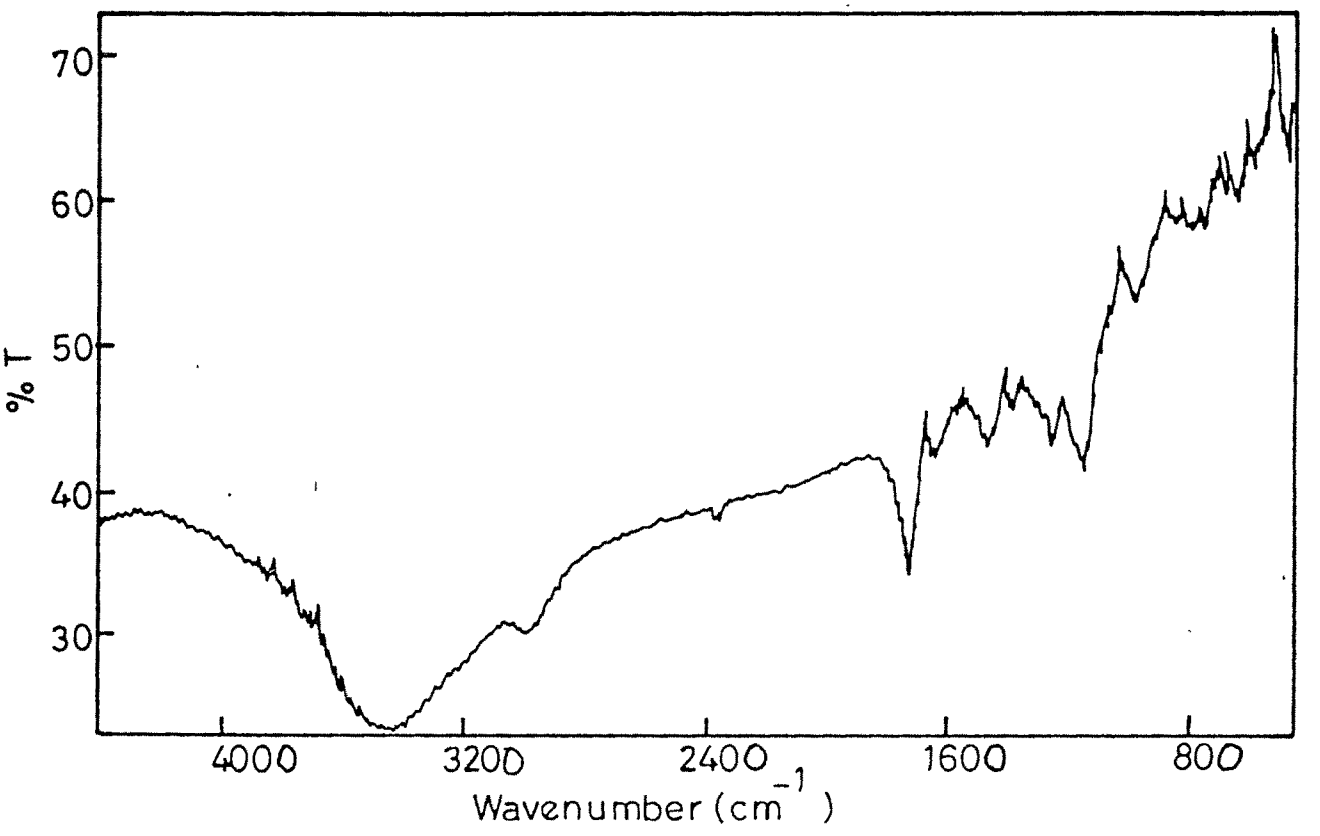

Fig. 3.19 FT-IR spectrum of the catalyst 8XPd(II)DAP

Table : 3.10

FTIR Frequency assignment for polymer bound ruthenium catalysts.

Catalyst	C-N Str (cm^{-1})	N-H Str (cm^{-1})	$-CH_2Cl$ Str (cm^{-1})
5PRu(III)DAP	1018	3420 1544	1264
15PRu(III)DAP	1040	3420 1634	1266
2XRu(III)DAP	1070	3440 1532	1262
8XRu(III)DAP	1150	3474 1538	1266

Table : 3.11

FTIR Frequency assignment for polymer bound palladium catalysts.

Catalyst	Pd-N Str (cm^{-1})	C-N Str (cm^{-1})	N-H Str (cm^{-1})	$-CH_2Cl$ Str (cm^{-1})
5PPd(II)DAP	475	1113	3415 1510	1265
15PPd(II)DAP	478	1120	3410 -	1268
2XPd(II)DAP	478	1150	3415 -	1267
8XPd(II)DAP	480	1150	3434 1574	1264

The NMR spectra of the unbound [Ru DAP Cl_2]Cl and 1,2-diamiopropane are recorded in deutero chloroform solution seperately.

The ligand (DAP) spectrum showed two peaks at 1.0δ and 2.42δ , which correspond to amino and methylene protons respectively. In the spectrum of [RuDAPCl_2]Cl the peaks due to methylene proton of DAP is shifted by 0.2 and the amino proton peak appears in the same region with multiple splitting (Figure 3.20) reflecting the different electronic environment of ligand after complexation. Integration of the peaks gave the correct number of protons present in the complex.

3.6.5 **Electron spectroscopy for chemical analysis (ESCA):**

Electron spectroscopy for chemical analysis (ESCA) also known as XPS (X-ray photoelectron spectroscopy) was introduced by Siegbahn and co-workers (13). This technique is currently one of the physical tools commonly employed in catalytic research (14). This is based on the famous principle of photoelectric effect invented by Einstein. In ESCA, a sample is irradiated by soft X-rays and the electrons knocked out from the various levels in the sample move with velocities depending on the binding energies. Since the binding energy of the core electron is a finger print of the atom, ESCA provides rapid elemental analysis. One can also get the information regarding the chemical state of an element from ESCA, due to the so-called "chemical shift"

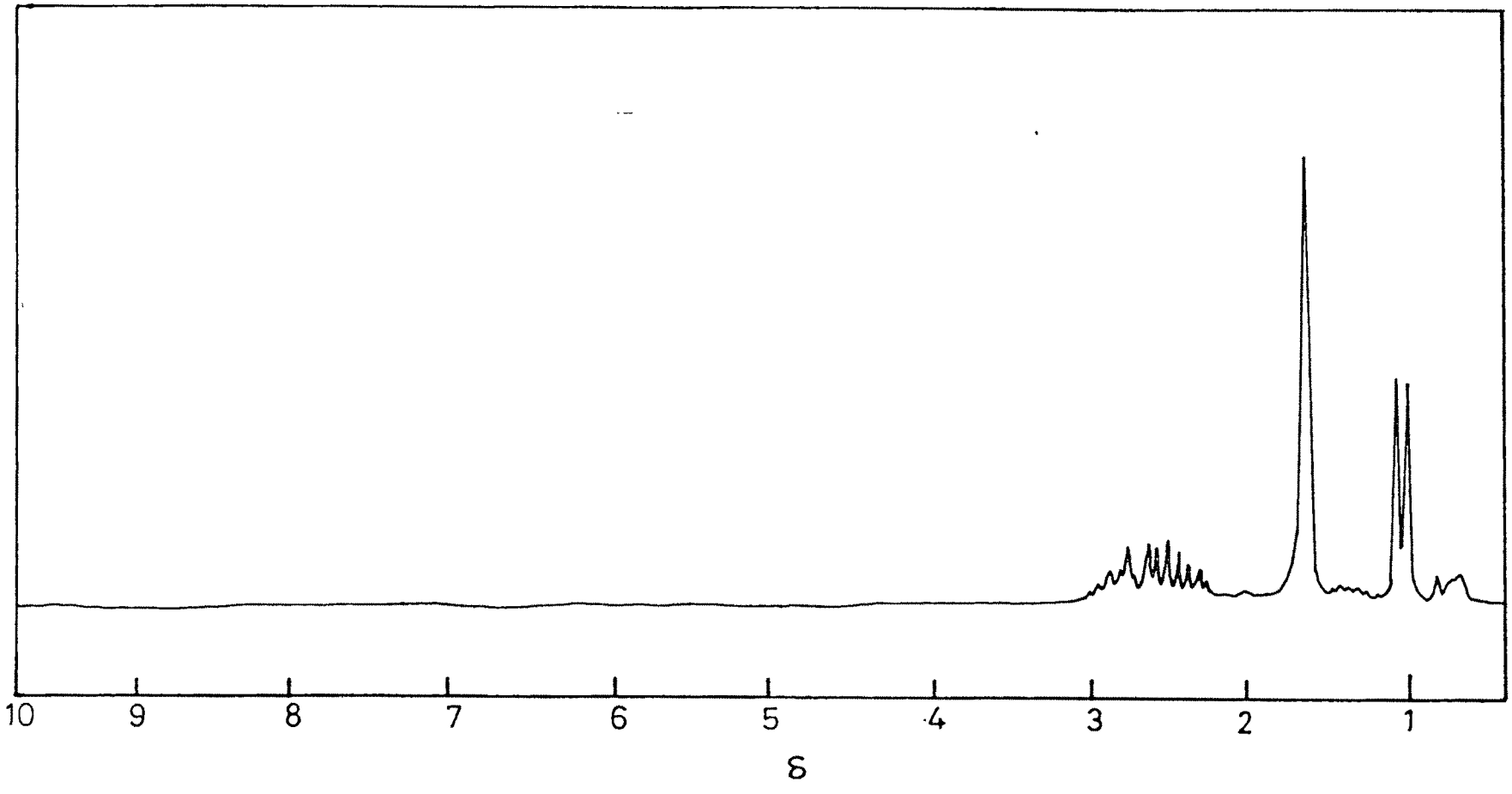

Fig. 3.20 NMR spectrum of unbound [$RuDAPCl_2$]Cl in $CDCl_3$

observed in photoelectron spectrum. This aspect of ESCA is particularly responsible for its extensive use in catalytic research (15).

ESCA studies of polymer bound ruthenium catalysts (Figs. 3.21 and 3.22) showed peaks due to Ru(3d 3/2) Ru(3p, 3/2), N(1s) Cl (2p 3/2) and C(1s) for ruthenium-DAP, indicating the +3 oxidation state of the metal. The broadening and shift of ESCA lines may be due to the different chemical environment of the polymer bound ruthenium complex (16). The intensity reversal is due to the super position (17) of C (1s) peak with Ru (3d 3/2).

The ESCA of polymer bound palladium catalyst (Fig. 3.23) showed peaks due to Pd (3p 3/2), Pd (3d 5/2) for palladium - DAP, indicating the +2 oxidation of the metal (18).

3.6.6 **Electron paramagnetic resonance (EPR) :**

EPR proves to be an ideal method to probe (i) g factor (ii) identification of paramagnetic species and (iii) for the characterization of environmental symmetry of the ion (19 - 22). For conducting EPR investigations a suitable paramagnetic probe, either intrinsic or extrinsic, should form a part of the system and this probe should not preferably perturb the environment. This technique finds wide application in the study of solid surfaces and in the identification of the surface species (23).

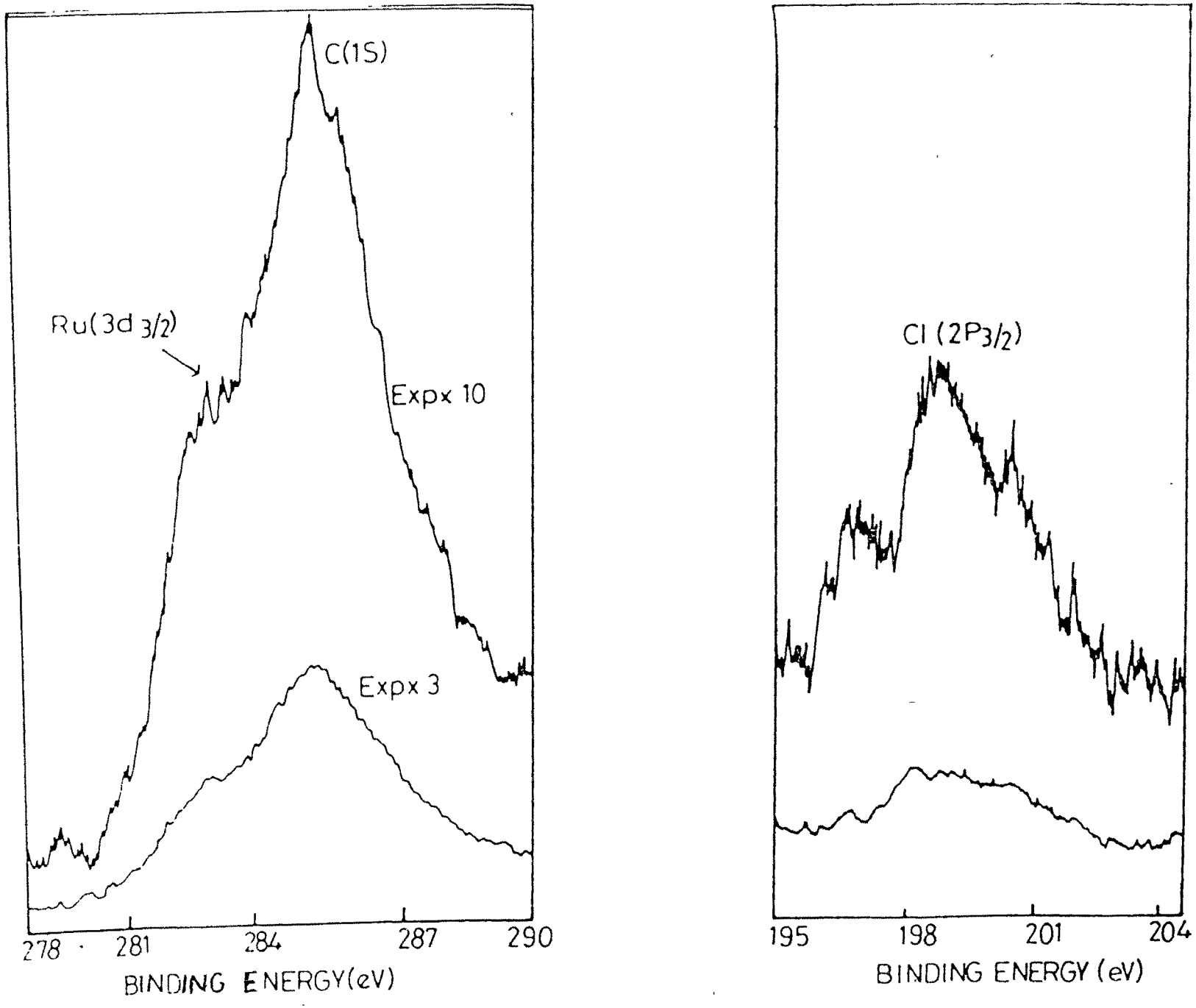

Fig. 3 21 ESCA spectra of 15PRu(III)DAP

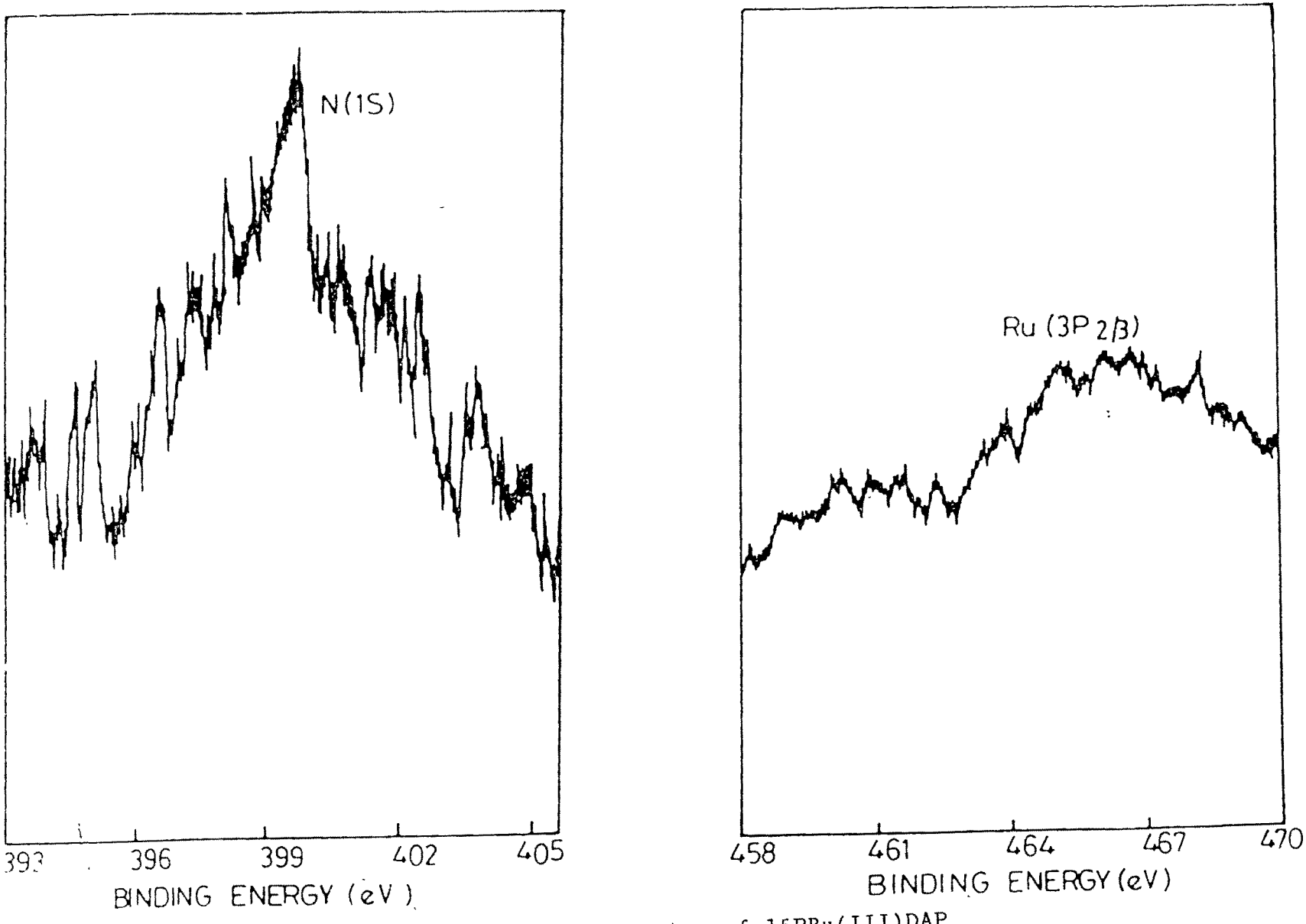

Fig. 3.22 ESCA spectra of 15PRu(III)DAP

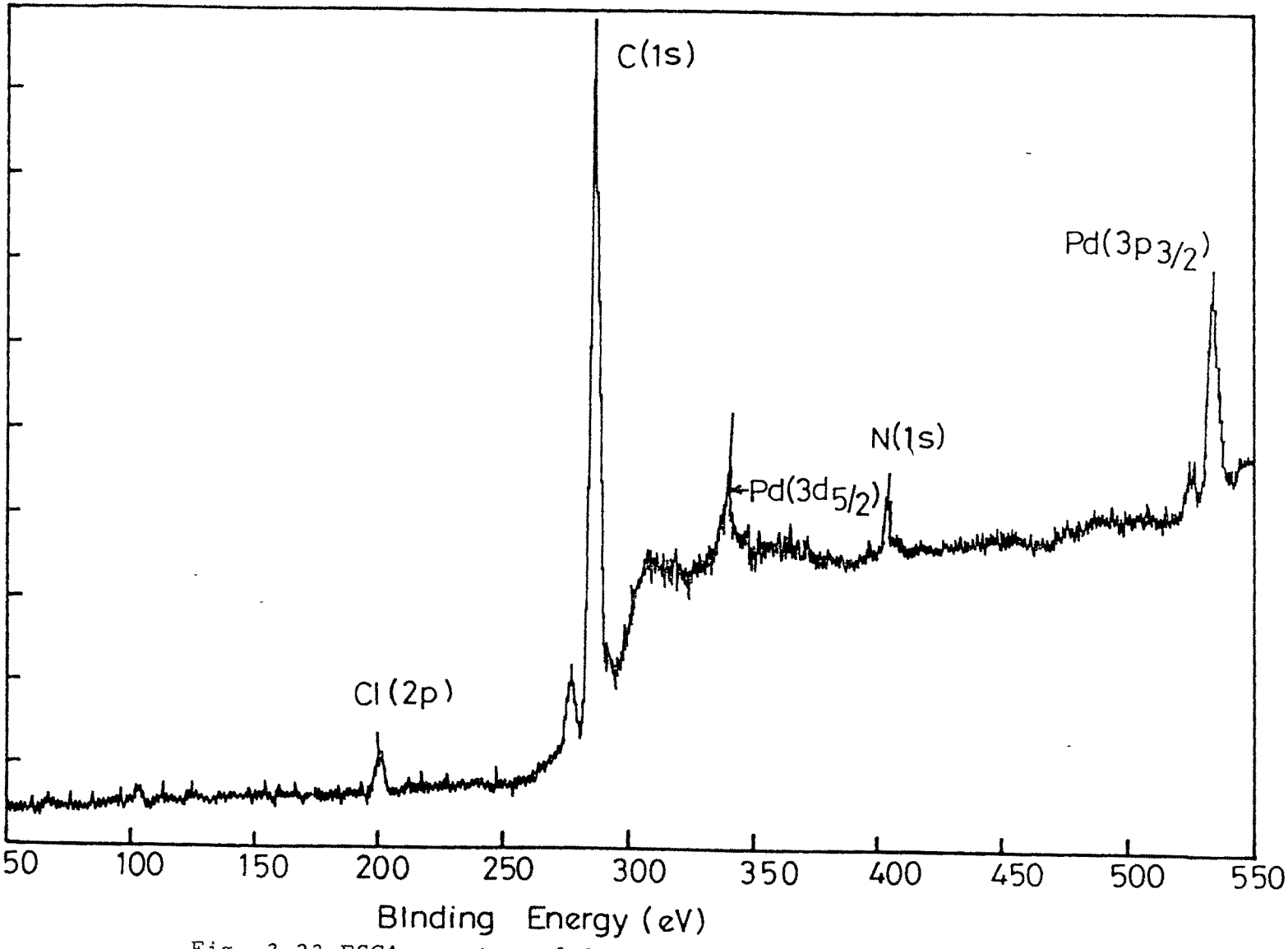

Fig. 3.23 ESCA spectra of 15PPd(II)DAP

Transition metal ions correspond to the widest and the most fruitful field of applications of EPR spectroscopy in heterogeneous catalysis. Some well studied ions include d^1 (Ti^{3+}, V^{4+}, Mo^{5+}), d^3 (V^{2+}, Cr^{3+}), d^5 (Mn^{2+}, Fe^{3+} Cr^{+}), d^7 (Co^{2+}, Pd^{3+}, Rh^{2+} in low spin form) and d^9 (Cu^{2+} Pd^{+}, Ag^{+}, Ni^{+}). These studies have wide range of applications including in surface sciences and catalysis as the ions with these configurations give EPR spectrum over a wide range of temperatures. (24).

EPR is essentially due to transitions between two energy levels of an unpaired electron, corresponding to two spin states in the presence of an external magnetic field. For a free electron which is not interacting with the surroundings, the transition energy is given by

$$\gamma h = \Delta E = g_e H\beta$$

Where h is the plancks constant, γ is the microwave frequency, β is the Bohrmagneton. H is the strength of the external magnetic field and g_e is the free electron with g - value equal to 2.0023. In the complexes g_e varies from the free electron environment in the molecule.

EPR spectrum of homogeneous catalyst [Ru(III)DAPCl$_2$]Cl is shown in Fig. 3.24. The g_I and g_{II} values were found to be 1.897 and 2.504 and g_{av} is 2.36. This is in agreement with a low spin d^3 centre in square planar environment, i.e., ruthenium is present in low - spin +3 oxidation state. Since the spectrum does not resemble a triplet state spectrum the

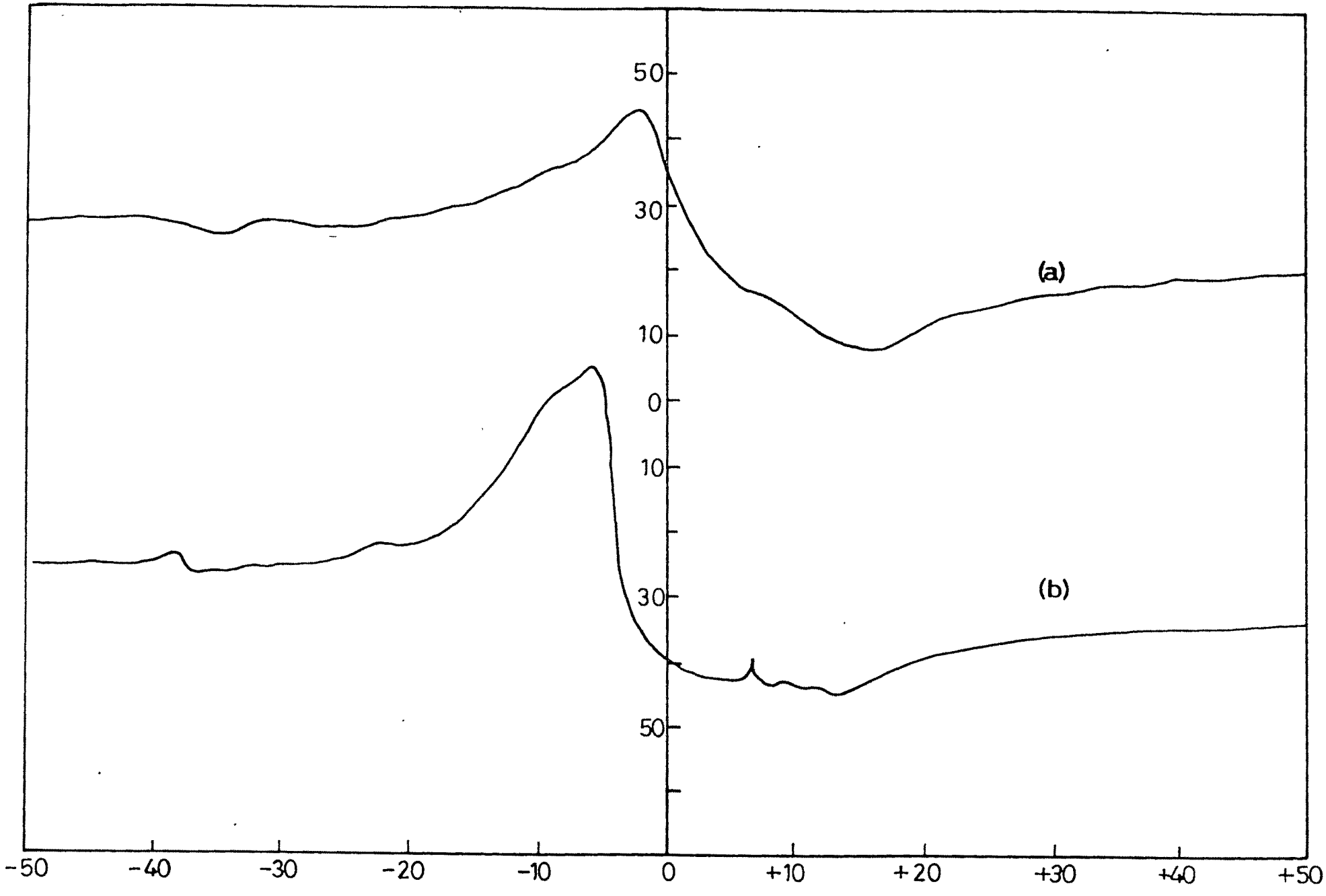

Fig. 3.24 EPR spectrum of homogeneous catalyst, $[RuDAPCl_2]Cl$ (a) Room Temp. (b) Liquid Nitrogen Temp.

possibility of Ru being in +4 oxidation state can be ruled out (low spin Ru(IV) will have two unpaired electrons). The possibility of Ru(II) may also be eliminated because it is diamagnetic and hence EPR inactive. Similar results have been reported by other workers for Ru (III) carbonyl complexes. (25 - 27)

Taquikhan et al. have studied the EPR spectrum of Ru (III) carbonyl chelates of schiff bases and average g value was obtained to be 2.1, confirming the presence of ruthenium in +3 oxidation state (28).

The higher magnitude g_{II} than g_{I} indicates that the ligand field in xy plane is stronger. In the present case this is possible only if the complex has the following structure.

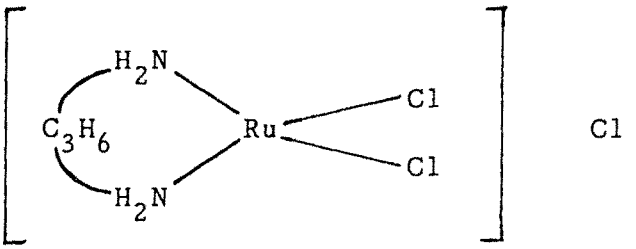

The EPR of unbound palladium complex, $[PdDAP]Cl_2$ was found to be inactive. This indicates the diamagnetic nature of the palladium (II) ion present in the species. It confirms that palladium is present in + 2 oxidation state.

3.7 **Morphology of polymer bound catalysts (SEM) :**

This technique allows essentially the imaging of the topography of a solid surface by use of back scattered or

secondary electrons (29). The scanning electron microscope is especially designed for the study of bulk samples. The low energy electrons (secondary electrons) provide topographical contrast, allowing study of the relief of the surface, whereas the high energy (back scattered) electrons give indications about variation in mean atomic weight across the specimen surface.

The behaviour of a catalyst depends upon the structure and composition of the active component as well as the morphology of its supporting medium. It can be determined on the basis of its structure at a range of magnification (from a few hundred to a few million times) which gives the information about the nature and the distribution of the active components, the nature of prorosity etc. The magnification in a simple electron microscopy is limitted, and extension of magnification by several order of magnitude is obtained with scanning electron microscope (SEM). The morphology of the catalyst can be studied with this technique (30).

Scanning electron micrographs of the polymer supports and polymer bound catalysts are shown in plates. 3.1 and 3.2. It was observed that the beads are porous and the texture changes with the change in the degree of crosslinking of polymer. A change in the shape of polymer beads has been found after anchoring the metal complexes. These changes are also revealed in surface area measurements.

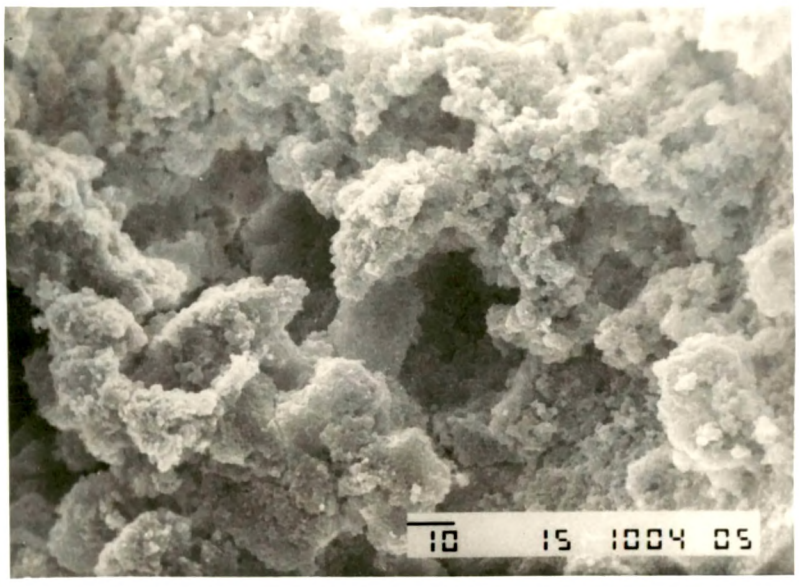

5P

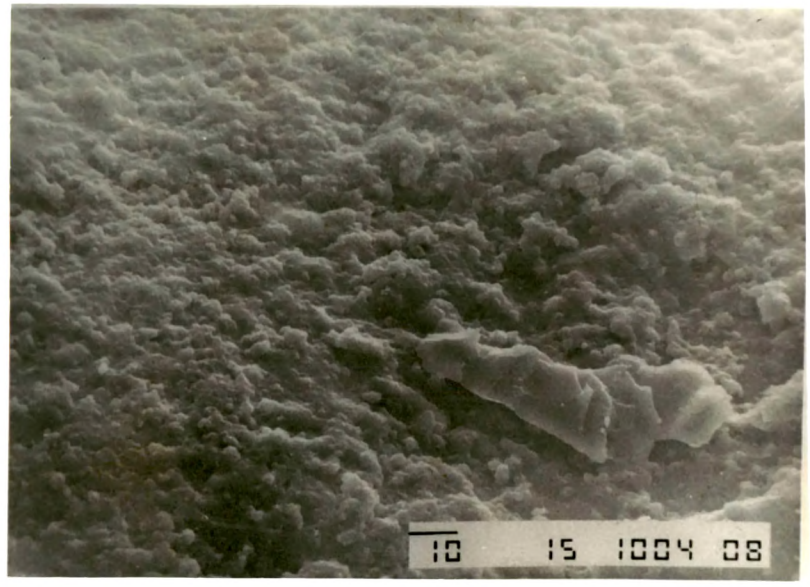

15P

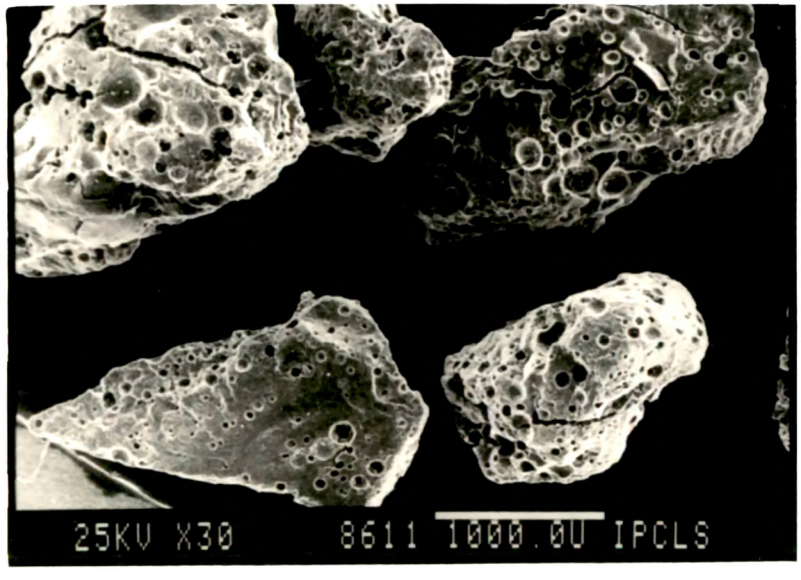

5PRu(III)DAP

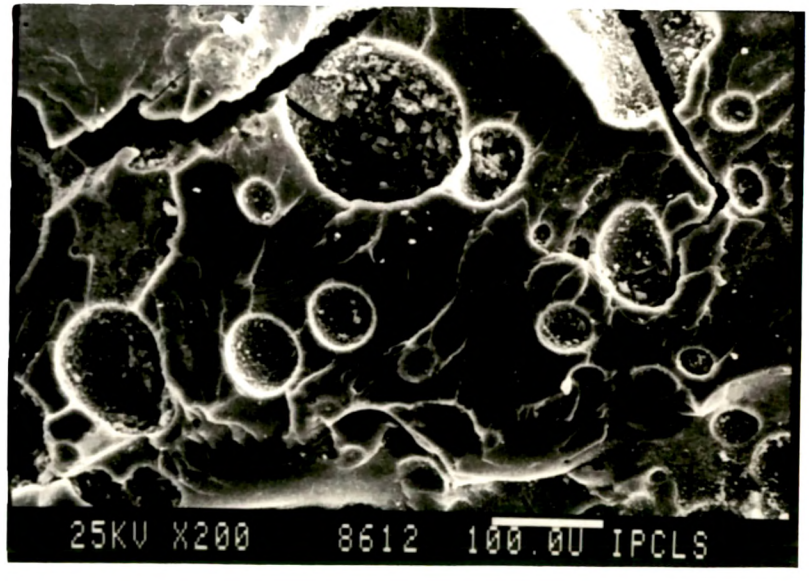

15P Ru(III)DAP

Plate. 3.1. Scanning electron micrographs of polymer supports and catalysts.

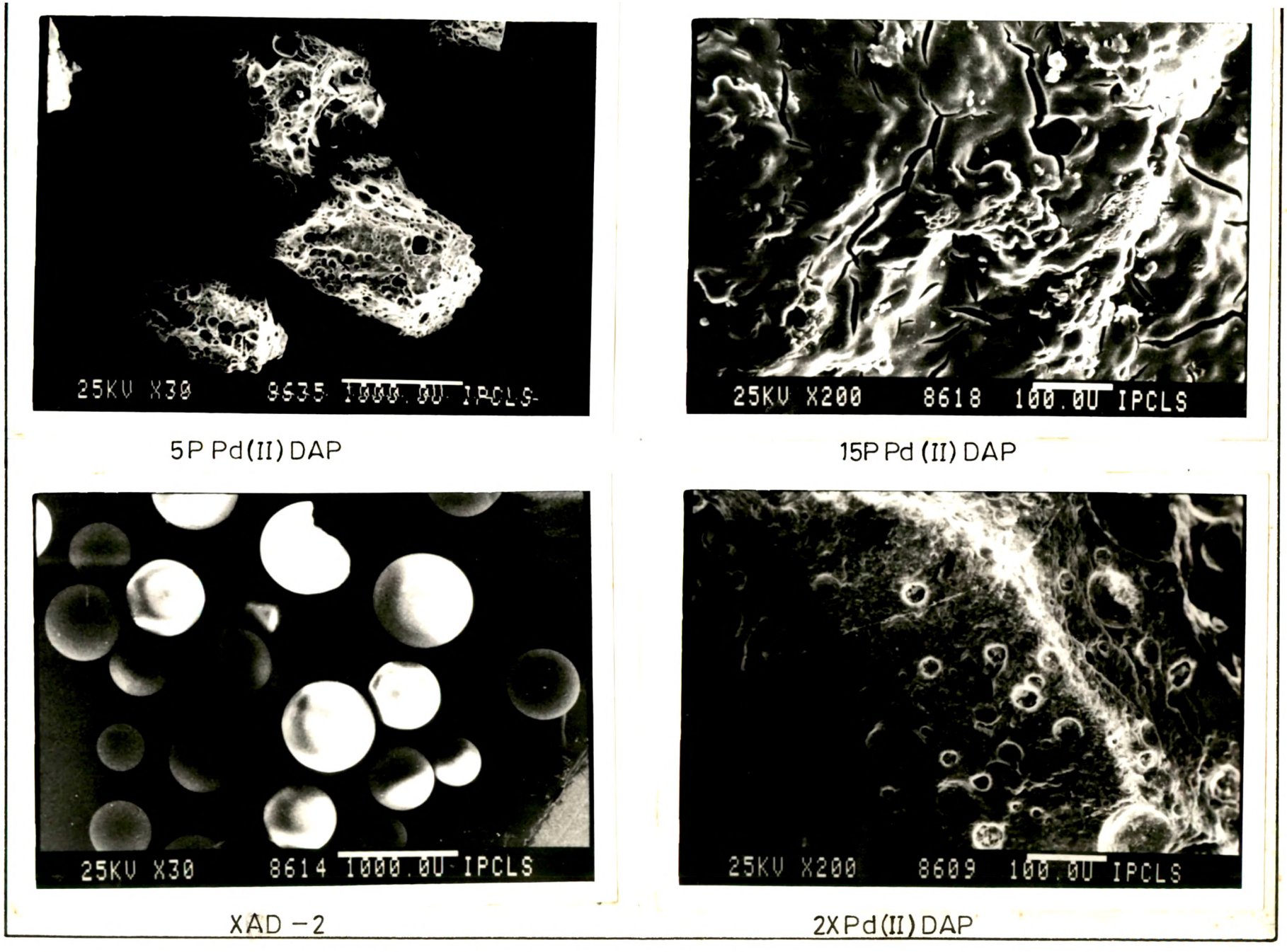

Plate. 3.2. Scanning electron micrographs of polymer supports and catalysts.

3.8 **Thermal stability :**

The change in weight and thermal property of a catalyst with changing experimental conditions can be used for a variety of studies. In the case of polymer bound metal complex catalysts weight loss or heat change may reveal the stability and phase change as a function of environment.

The thermal stability of many metal complex catalysts (31 - 34) was found to be enhanced when supported on inorganic oxides or polymers. Since the thermal properties and other properties of the polymer support vary with the crosslinking of the polymer, the micro environment around the metal ion changes co-ordination sphere of the metal ion induced by complex formation on the polymer matrix, which further leads to special stability of the metal complex. Hence, the study of thermal behaviour of the polymer support, unbound metal complex and polymer bound metal complex will be useful to determine the limit of the catalytic reaction temperature.

3.8.1 **Thermal stability of the support :**

Since the support used was hydrophobic, they are found to be stable upto 150^{o} C and the degradation starts above 200^{o} C. Fig. 3.25 shows TGA of poly (Sty- DVB) support used for the synthesis of the catalyst. The supports can be used very safely upto 100^{o} C.

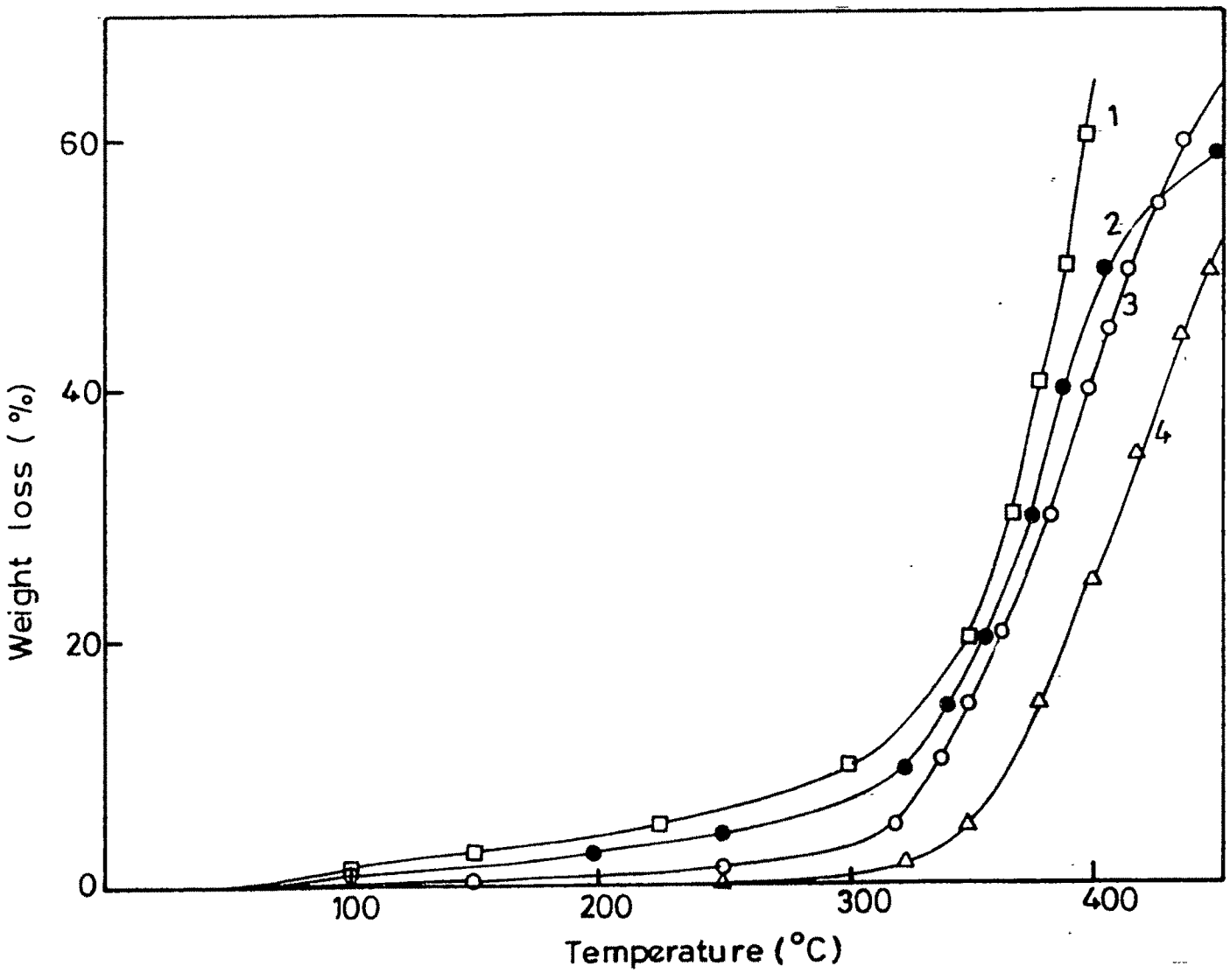

Fig. 3.25 Thermogravimetric curves of polymer supports

1. XAD-2 2. XAD-8 3. 5P 4. 15P

It was found that as the crosslinking increases, the thermal stability of the polymer also increases. The weight loss may be due to the evaporation of organic matter entrapped inside the fine pores.

3.8.2 Thermal stability of the catalysts :

Fig. 3.26 shows the DTA and TG curves for unbound Ruthenium and palladium complexes. It may be noted that metal complex is stable upto $\simeq 200^{\circ}$ C. Above this temperature metal complex changes its phase. This is reflected from the endothermic DTA peaks. The intial weight loss is due to moisture content. TGA curves for polymer supported catalysts are shown in figures 3.27 and 3.28. A change is observed in the thermal stability of the catalysts after supporting the metal ions onto the polymer surface.

From the thermal stability studies it can be concluded that all the polymer anchored catalysts in the present investigation may be employed safely below 100°C. The initial weight loss is due to the moisture present in the catalysts.

From all the above physico chemical characterization and spectroscopic evidences the following probable structures of polymer bound catalysts have been proposed.(Scheme.3.1)

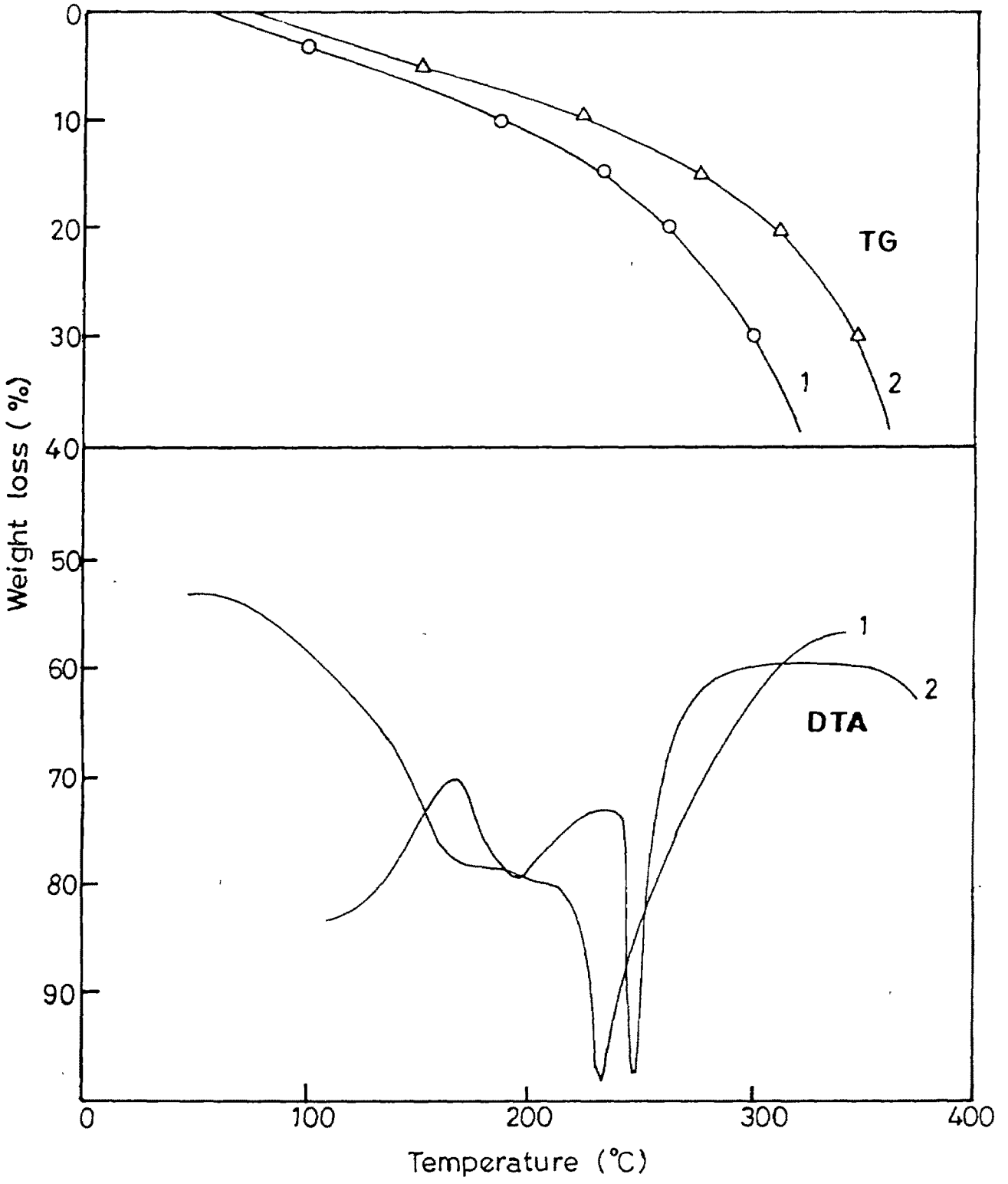

Fig. 3.26 DTA/TG curves of unbound complexes
1. $[RuDAPCl_2]Cl$ 2. $[PdDAP]Cl_2$

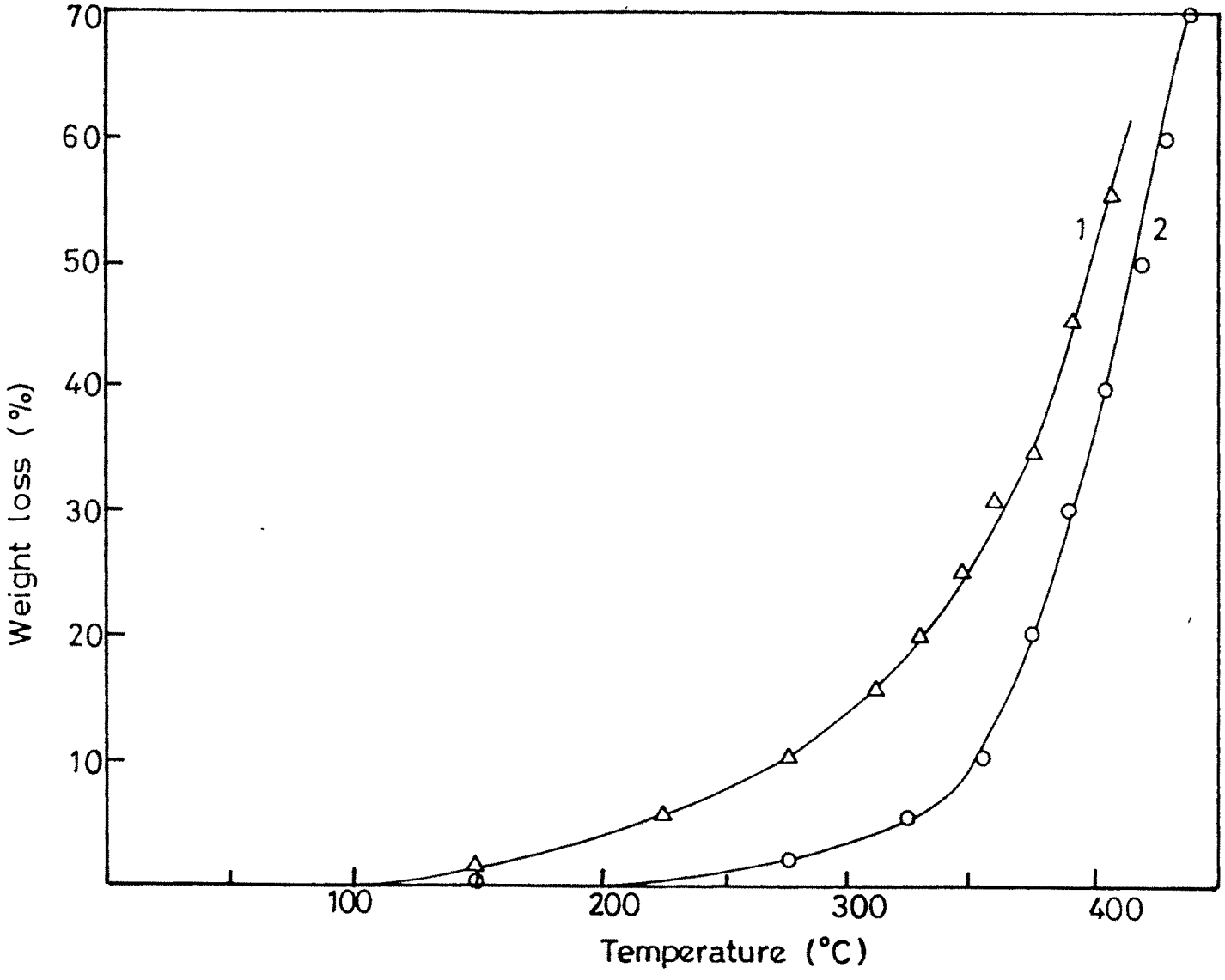

Fig. 3.27 Thermogravimetric curves of polymer supported catalysts
1. 5PRu(III)DAP 2. 15PRu(III)DAP

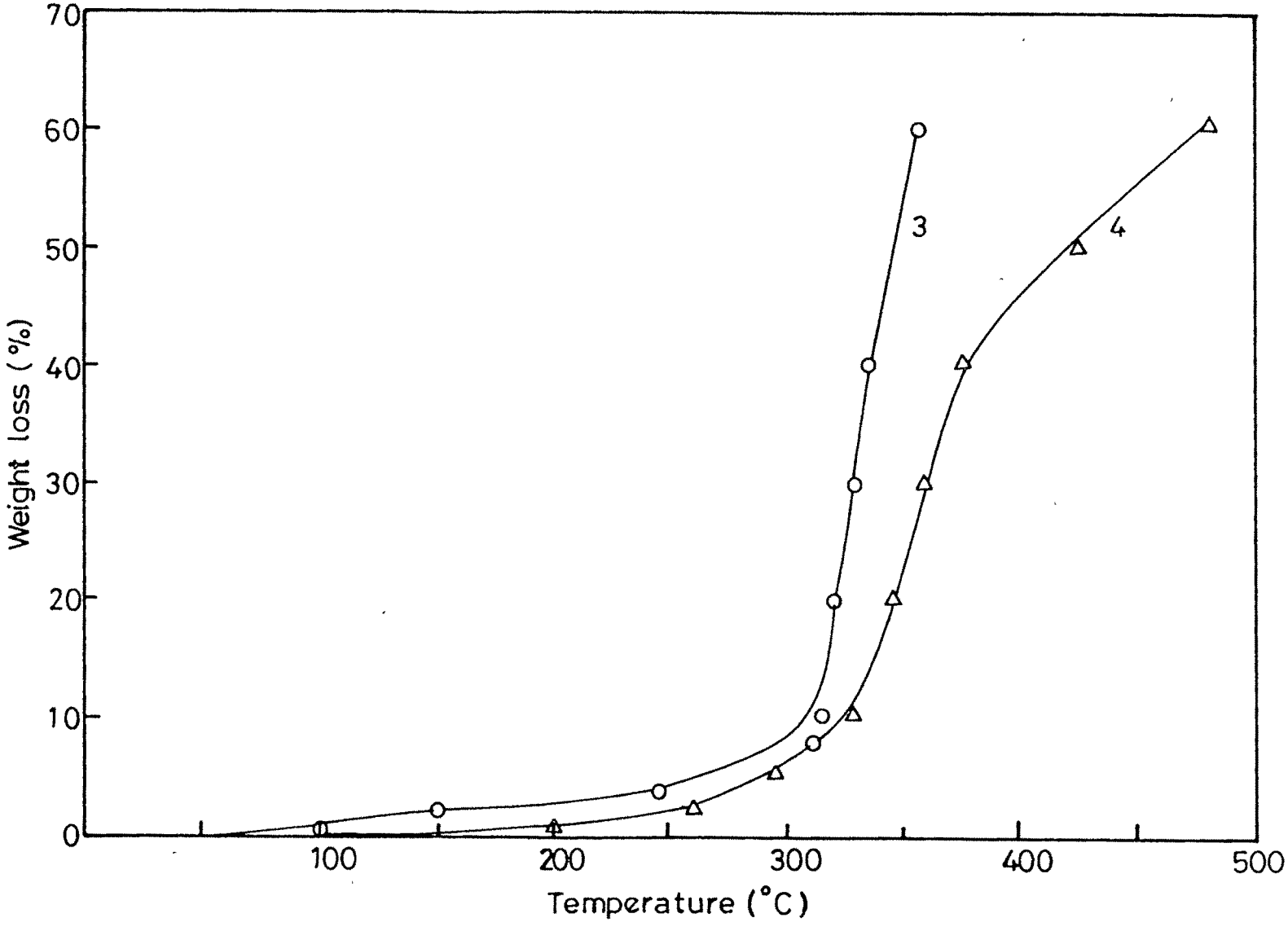

Fig. 3.28 Thermogravimetric curves of polymer supported catalysts
3. 8XPd(II)DAP 4. 2XRu(III)DAP

SCHEME . 3.1

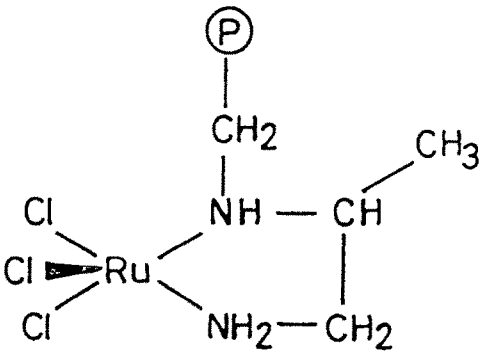

I

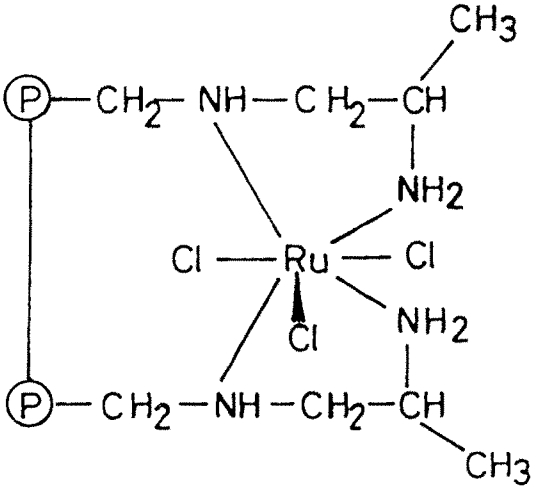

II

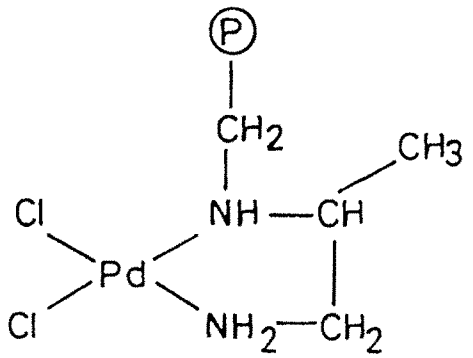

III

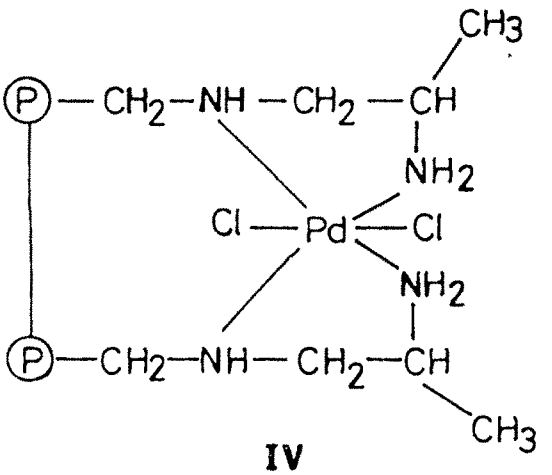

IV

3.9 References :

1. F.W. Billmeyer : Textbook of polymer science, Wiley Inter science, New york, Third Edition (1979).
2. R. B. Seymour : Introduction to polymer chemistry McGraw - Hill, New york (1971).
3. R. Kunin, "Ion Exchange Resins" John Wiley and Sons Ltd (1958).
4. D. M. Yoing and A.D.Crowell, "Physical Adsorption of gases" Butter Worths, London (1962).
5. S. J. Gregg and K. S. W. Sing, "Adsorption, Surface area and porosity", Academic press London (1967).
6. K. Klier, Catal. Rev., 1,207, (1967).
7. G. Kortum, "Reflectance Spectroscopy, Principles, Methods, and Application"; Springer-Verlag Berlin (1969).
8. W. N. Delgass, G.L.Haller, R. Kellerman and J.H. Lunsford, "Spectroscopy in Heterogeneous catalysis", Chapter-4, Academic Press, New York (1979).
9. W. W. Wendlandt and H. G. Hecht, "Relfectance Spectroscopy," Wiley Inter Sci, New York (1966).
10. E. Seddon and K. Seddon, "The Chemistry of Ruthenium" Elsevier, Amsterdam (1984).
11. Y. Kurimura, E.. Isuchida and M. Kaneho, J. Polym. Sci., A (I) 9, 3521 (1971).
12. J. Roda; Makromol. Chem; 178, 203, (1977).

12a. P. R. Griffiths and J. A. Dettaseth in Fourier Transform Infrared Sepctrometry, Wiley Inter Science, New York, 1986.

13. K. Siegbahn, C. Nordling, A. Fahlman, R. Nordberg, K. Hamrin, J. Hedman, G. Johansson, T. Bergmark, S.E. Karlsson, I. Lindgren, and B. Lindberg; in ESCA : Atomic, Molecular and Solid state Structure studied by Means of Electron spectroscopy. Nova Acta Regiae Soc. Sci. Uppsaliensis, Ser. IV Vol 20.

14. W. N. Delgass, T. R. Hygies, and C.S.Fadley, Catal. Rev., 4, 179, (1970).

15. P. S. Murty in "Spectroscopic Methods in Heterogeneous Catalysis" Eds. N. M. Gupta, V.B.Kartha and R.A.Rajadyaksha; Tata McGraw Hill Publ Co. Ltd., New Delhi India, p.167 (1991).

16. M. M. Taqui Khan, S.A. Samad and M. R. H. Siddiqui; J. Mol catal; 50 97 (1989).

17. D. K. Chakrabarty, P. K. Basu, A Patil, N. Ramachandran and P. Prabhawalkar; Advances in catalysis, Science and Technology", Ed. T.S.R. Prasada Rao; Wiley Eastern Ltd., New Delhi, India (1985).

18. Joice P. Mathew and M. Srinivasan Chemistry and Industry (London) 8,262-3 (1990).

19. J. C. Vedrine in "Characterization of Heterogeneous Catalysts" Ed., F. Delannay, Marcel Dekker Inc., New York (1984).

20. B. A. Goodman and J. B. Raynor, Adv. Inorg. Chem. Radio Chem., 13 : 135 (1979).

21. R. D.. Dowsing and J. F. Gibson, J. Chem. Phys,50 : 294 (1969).

22. M. Che, J.. Fraissard, and J. C. Vedrine, Bull. Groupe, Fr. Argiles, 26 : 1 (1974)..

23. J. Reed, P. Eisenberger, B. K. Teo and B. M. Kincaid, J. Am. Chem. Soc, 100 2375 (1978).

24. M. S. Sastry in "Spectroscopic Methods in Heterogeneous Catalysis", Eds. N. M. Gupta, V.B. Kartha and R.A.. Rajadhyaksha, Tata, McGraw Hill Publ. Ltd., New Delhi India, (1991).

25. A. Hudson and M. J. Kennedy; J. Chem. Soc. (A), 1169, (1969).

26. B. L. Gustafson, M. J. Lin and J. H. Lunsford, J. Phys. Chem; 84, 3211 (1980).

27. S. Sasaki, Y. Yanase, N. Hagiwara, T. Takeshila, H. Naganuma, A Ohyoshi, and K. Ohkubo, J. Phys. Chem. Soc., 86, 1038, (1982).

28. M. M. Taquikhan, D. Srinivas, R. I. Kureshy and N. H. Khan; Inorg. Chem. 29, 2320 (1990).

29. J. I. Goldstein and H. Yakowitz Eds "Practical Scanning Electron" Plenum Press, New York (1975).

30. J. V. Sanders in "Catalysis, Science and Technology," Eds. J. R. Anderson and M. Boudart, Springer - Verlag, Berlin, Heidelberg, Vol;. 7, p - 51, (1985).

31. L. Jinxing. Y. Lixin. G.. Shivrying, H. Lijuan, I. Renyuan and L. Dongbai, Thermochimica Acta; 123 121 (1988).

32. N. L. Holy; J. Org. Chem; 44, 239, (1979).

33. N. L. Holy, in "Fundamental Research in Homogeneous Catalysts" Ed. M. Isutsui, Plenum Press, New York, 3 691 (1979).

34. J. Sestak, V. Satara, and W. W. Wendlandt, Thermochim, Acta, 7, 333 (1973).